

# Blind analysis of isobar data for the CME search by the STAR collaboration

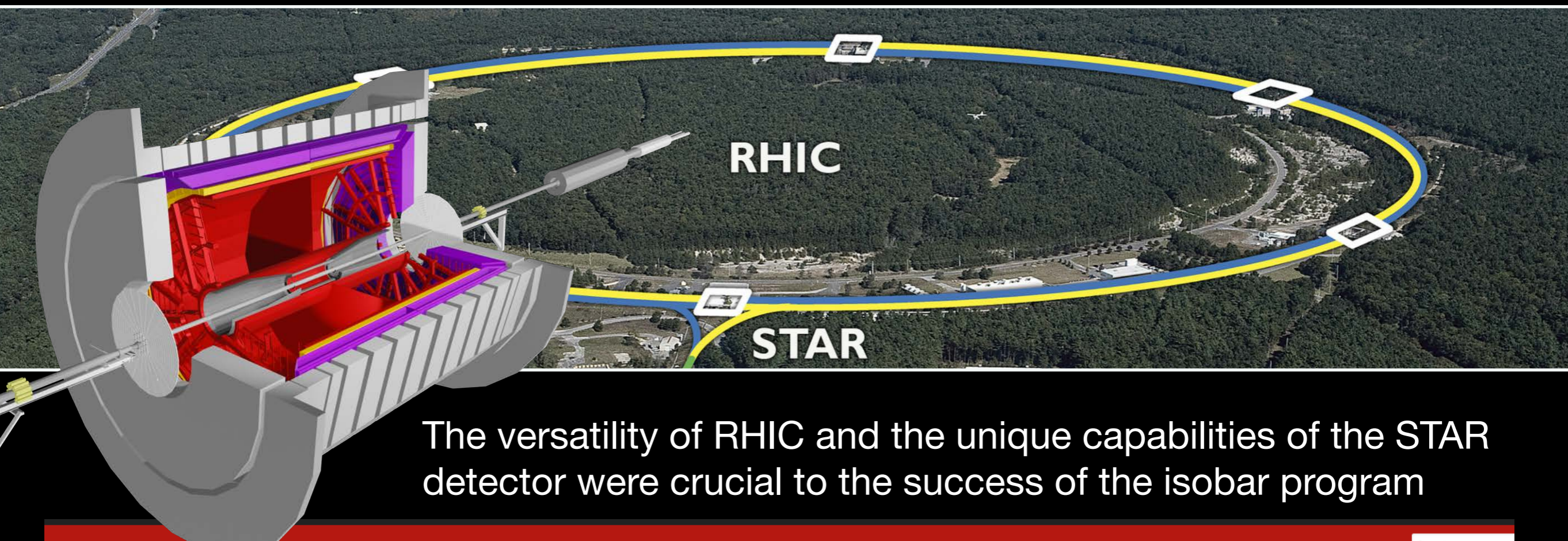
Prithwish Tribedy  
(Brookhaven National Laboratory)



RBRC seminar, Sept 2, 2021

Based on: <https://arxiv.org/abs/2109.00131>

# Isobar program: long journey since early 2018



The versatility of RHIC and the unique capabilities of the STAR detector were crucial to the success of the isobar program

arXiv.org > nucl-ex > arXiv:2109.00131

Search...

Help | Advanced Search

## Nuclear Experiment

[Submitted on 1 Sep 2021]

### Search for the Chiral Magnetic Effect with Isobar Collisions at $\sqrt{s_{NN}} = 200$ GeV by the STAR Collaboration at RHIC

STAR Collaboration: M. S. Abdallah, B. E. Aboona, J. Adam, L. Adamczyk, J. R. Adams, J. K. Adkins, G. Agakishiev, I. Aggarwal, M. M. Aggarwal, Z. Ahammed, I. Alekseev, D. M. Anderson, A. Aparin, E. C. Aschenauer, M. U. Ashraf, F. G. Atetalla, A. Attri, G. S. Averichev, V. Bairathi, W. Baker, J. G. Ball Cap, K. Barish, A. Behera, R. Bellwied, P. Bhagat, A. Bhasin, J. Bielcik, J. Bielcikova, I. G. Bordyuzhin, J. D. Brandenburg, A. V. Brandin, I. Bunzarov, X. Z. Cai, H. Caines, M. Calderón de la Barca Sánchez, D. Cebra, I. Chakaberia, P. Chaloupka, B. K. Chan, F.-H. Chang, Z. Chang, N. Chankova-Bunzarova, A. Chatterjee, S. Chattopadhyay, D. Chen, J. Chen, J. H. Chen, X. Chen, Z. Chen, J. Cheng, M. Chevalier, S. Choudhury, W. Christie, X. Chu, H. J. Crawford, M. Csanád, M. Daugherty, T. G. Dedovich, I. M. Deppner, A. A. Derevschikov, A. Dhamija, L. Di Carlo, L. Didenko, P. Dixit, X. Dong, J. L. Drachenberg, E. Duckworth, J. C. Dunlop, N. Elsey, J. Engelage, G. Eppley, S. Esumi, O. Evdokimov, A. Ewigleben, O. Eyser, R. Fatemi, F. M. Fawzi, S. Fazio, P. Federic, J. Fedorisin, C. J. Feng, Y. Feng, P. Filip, E. Finch, Y. Fisyak, A. Francisco, C. Fu, L. Fulek, C. A. Gagliardi, T. Galatyuk, F. Geurts, N. Ghimire, A. Gibson, K. Gopal, X. Gou, D. Grosnick, A. Gupta, W. Guryn, A. I. Hamad et al. (298 additional authors not shown)

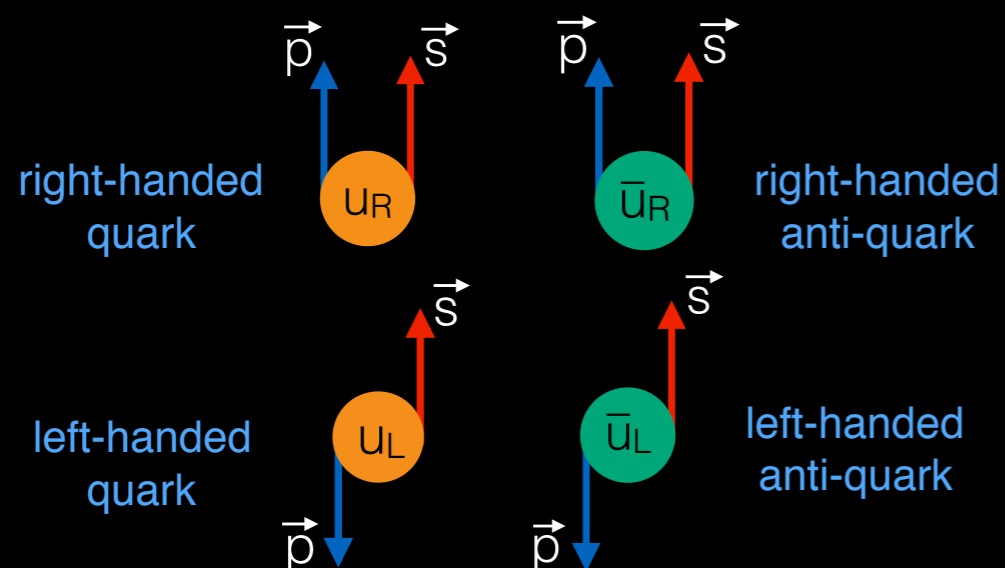
The chiral magnetic effect (CME) is predicted to occur as a consequence of a local violation of  $\mathcal{P}$  and  $\mathcal{CP}$  symmetries of the strong interaction amidst a strong electro-magnetic field generated in relativistic heavy-ion collisions. Experimental manifestation of the CME involves a separation of positively and negatively charged hadrons along the direction of the magnetic field. Previous measurements of the CME-sensitive charge-separation observables remain inconclusive because of large background contributions. In order to better control the influence of signal and backgrounds, the STAR Collaboration performed a blind analysis of a large data sample of approximately 3.8 billion isobar collisions of  $^{96}_{44}\text{Ru}+^{96}_{44}\text{Ru}$  and  $^{96}_{40}\text{Zr}+^{96}_{40}\text{Zr}$  at  $\sqrt{s_{NN}} = 200$  GeV. Prior to the blind analysis, the CME signatures are predefined as a significant excess of the CME-sensitive observables in Ru+Ru collisions over those in Zr+Zr collisions, owing to a larger magnetic field in the former. A precision down to 0.4% is achieved, as anticipated, in the relative magnitudes of the pertinent observables between the two isobar systems. Observed differences in the multiplicity and flow harmonics at the matching centrality indicate that the magnitude of the CME background is different between the two species. No CME signature that satisfies the predefined criteria has been observed in isobar collisions in this blind analysis.

Comments: 43 pages, 27 figures

Subjects: Nuclear Experiment (nucl-ex); High Energy Physics - Experiment (hep-ex); High Energy Physics - Phenomenology (hep-ph); Nuclear Theory (nucl-th)

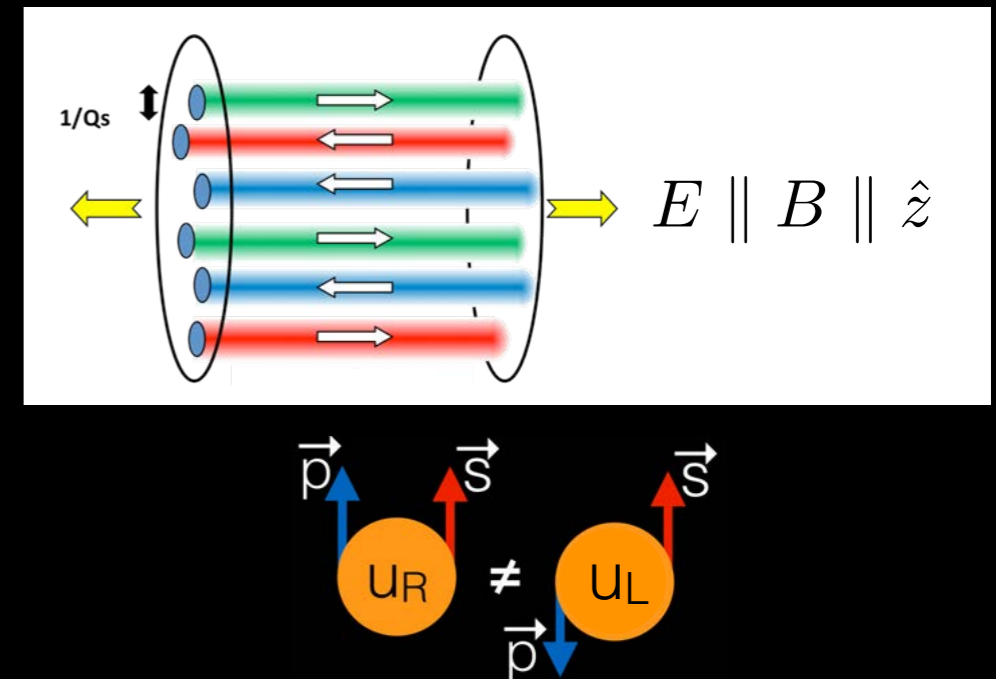
# Chirality Key players in the game

1 Deconfined medium of massless quark (chiral symmetry restored)



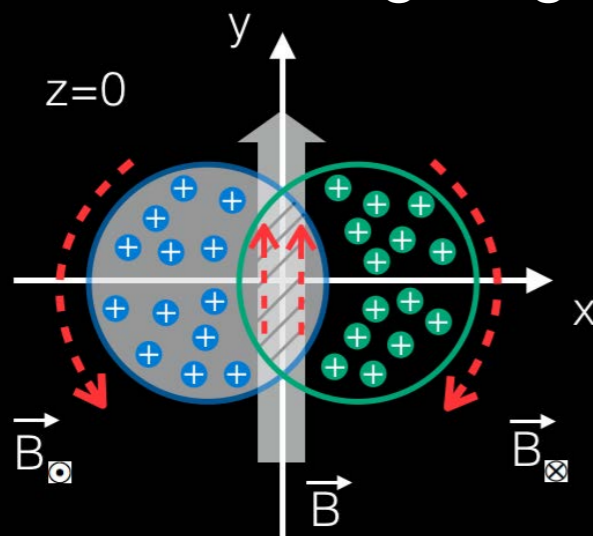
Kharzeev, McLerran, Warringa 0711.0950

2 Mechanism to create imbalance of left & right handed quarks



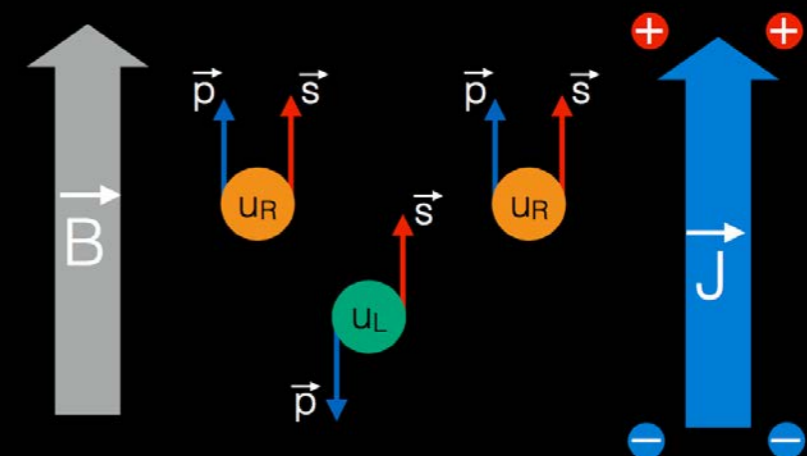
Kharzeev et al, hep-ph/0109253, Mace et al, 1601.07342, Muller et. al.1606.00342, Lappi et al,1708.08625

3 Presence of a strong magnetic-field



Kharzeev et al 0711.0950, Skokov et al 0907.1396, McLerran et al 1305.0774

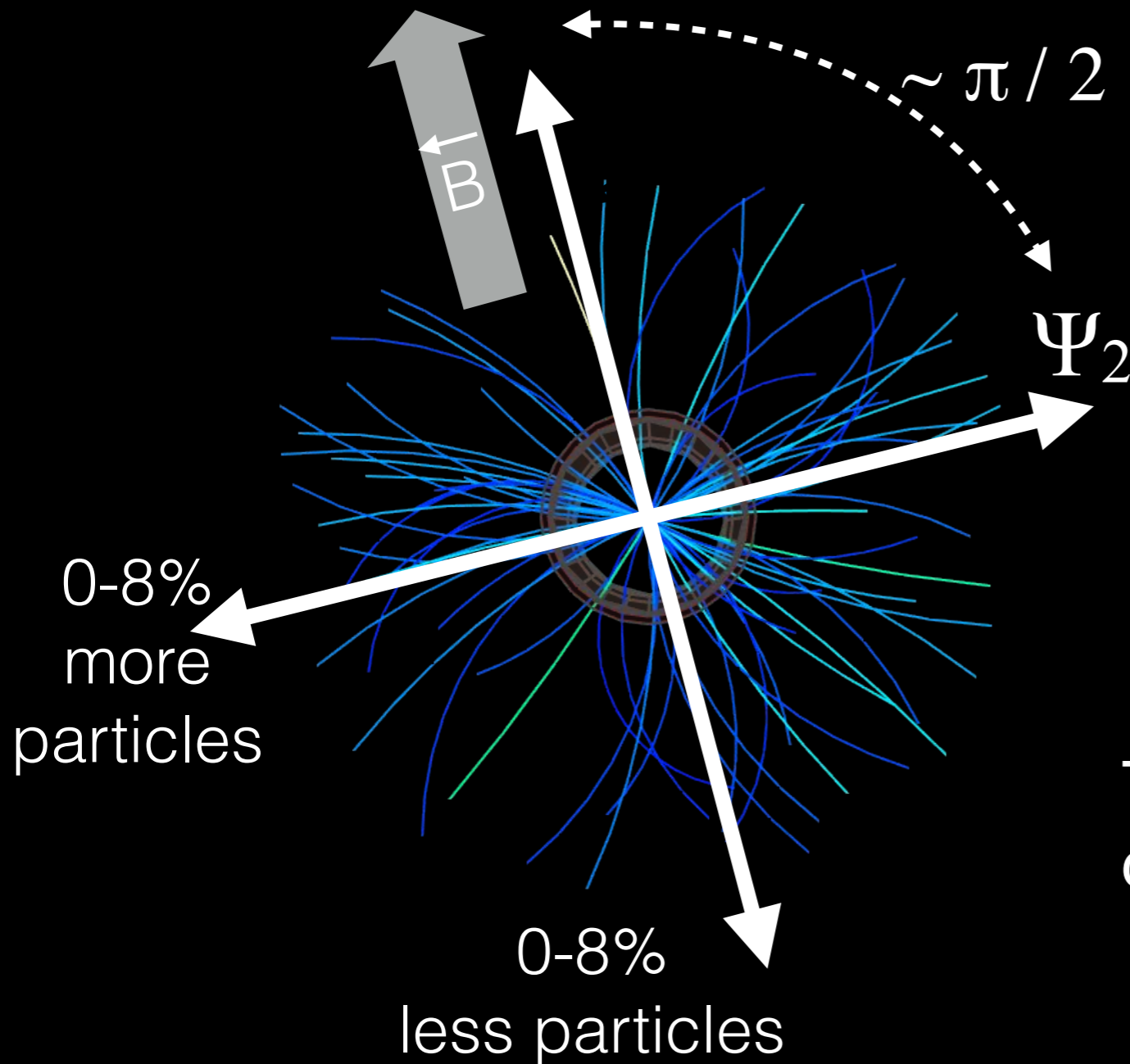
4 Chiral Magnetic Effect ( $J \parallel B$ )



Kharzeev, arXiv:hep-ph/0406125

# How do we detect it : find B-field direction

Elliptic anisotropy is measured by correlation between two particles



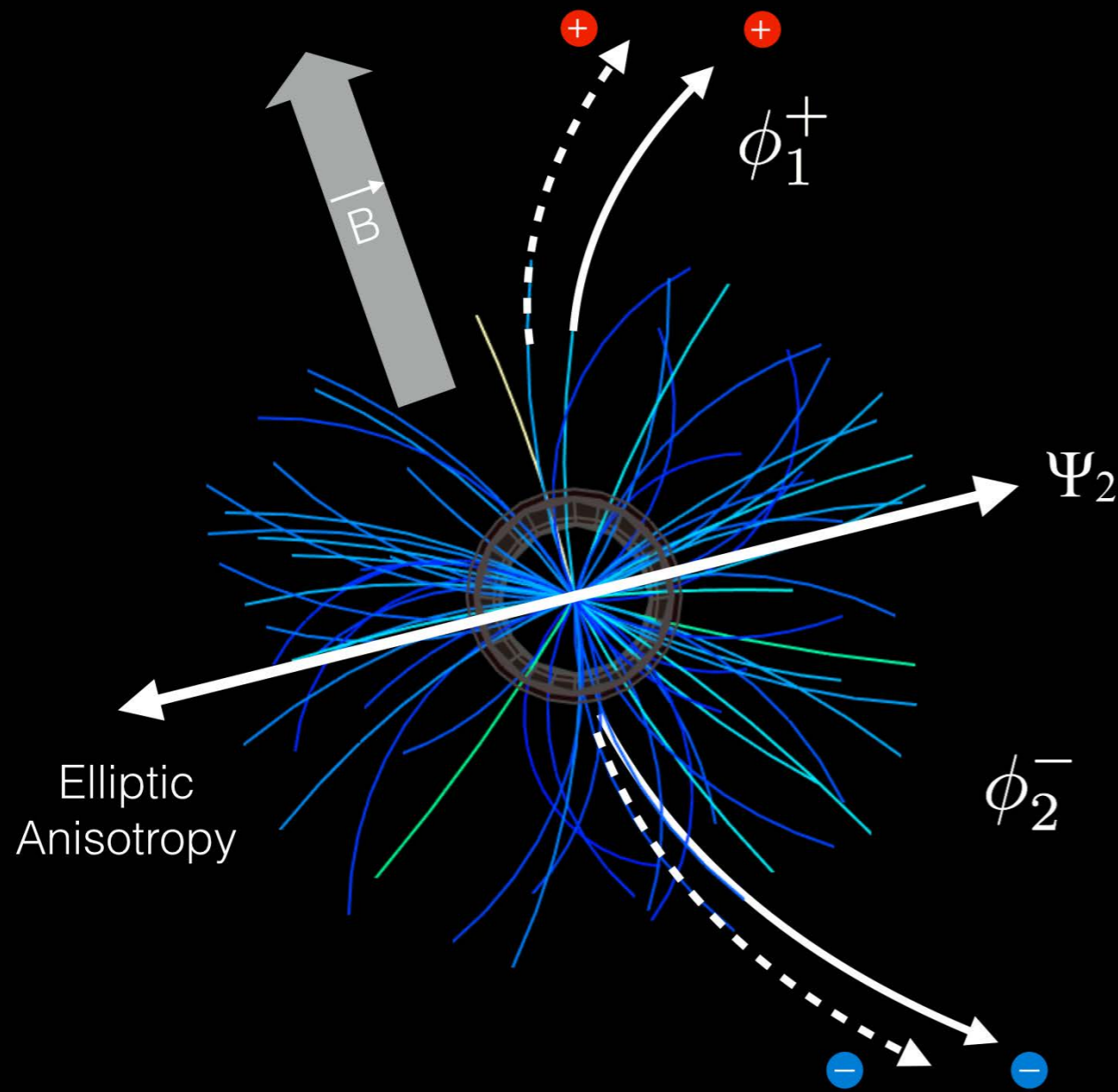
$$v_2\{EP\} = \langle \cos(2\phi_1 - 2\Psi_2) \rangle$$

$$v_2\{2\}^2 = \langle \cos(2\phi_1 - 2\phi_2) \rangle$$

The plane of elliptic anisotropy  $\Psi_2$  is correlated to B-field direction

# How do we detect it : measure charge separation

Measure charge separation across  $\Psi_2$  using the correlator:



$$\gamma^{\alpha,\beta} = \langle \cos(\phi_1^\alpha + \phi_2^\beta - 2\Psi_2) \rangle$$

CME case :  $\gamma^{SS} \neq \gamma^{OS}$

$$\gamma^{+-} = \cos(\pi/2 - \pi/2 + 0) = 1$$

$$\gamma^{++,- -} = \cos(\pi/2 + \pi/2 + 0) = -1$$

Quantity of interest:

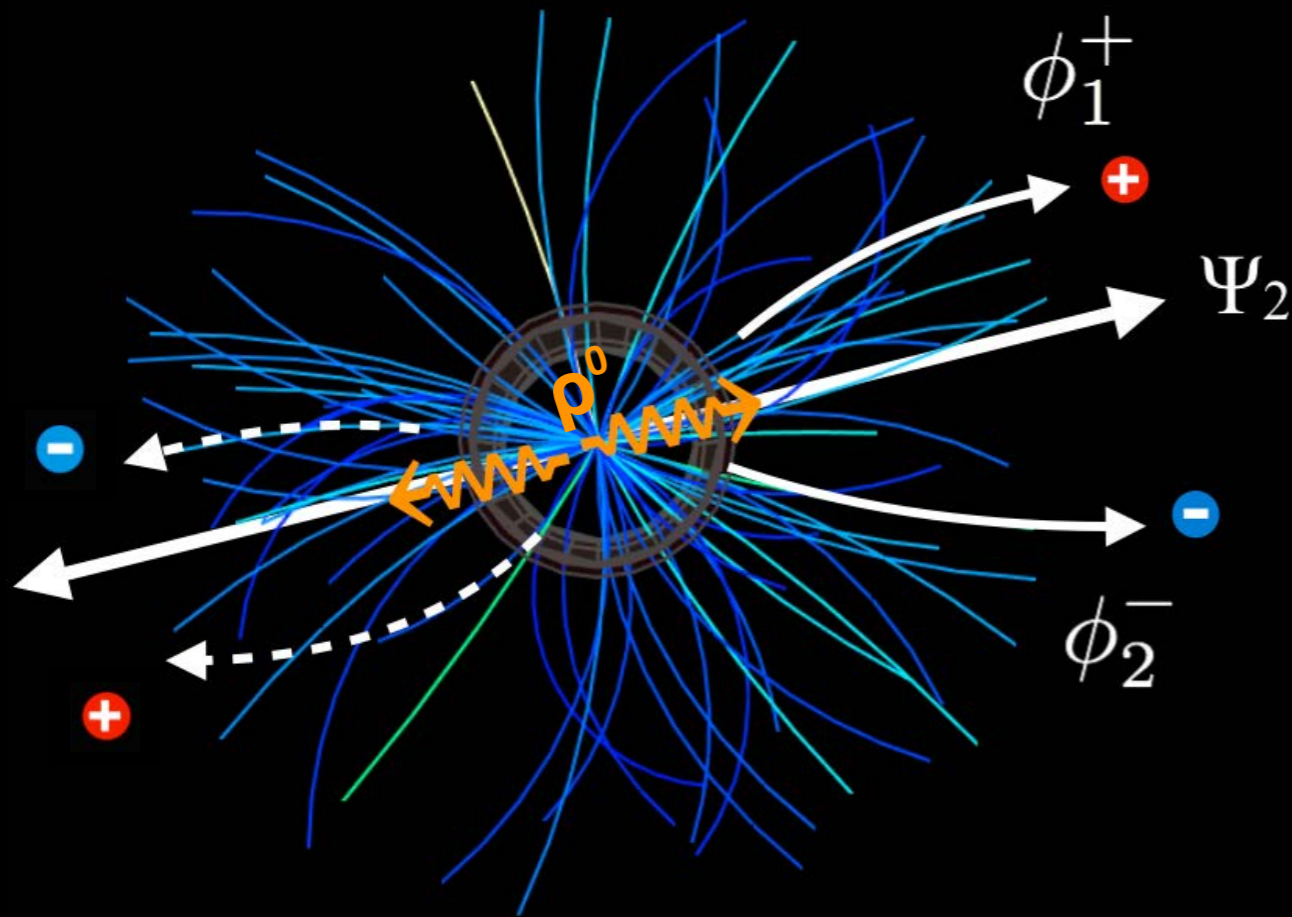
$$\Rightarrow \Delta\gamma^{CME} = \gamma^{OS} - \gamma^{SS} > 0$$

Voloshin, hep-ph/0406311

CME causes difference in opposite-sign & same-sign correlation

# How do we detect it : measure charge separation

Measure charge separation across  $\Psi_2$  using the correlator:



$$\gamma^{\alpha,\beta} = \langle \cos(\phi_1^\alpha + \phi_2^\beta - 2\Psi_2) \rangle$$

Flowing  
resonance decay:  $\gamma^{ss} \neq \gamma^{os}$

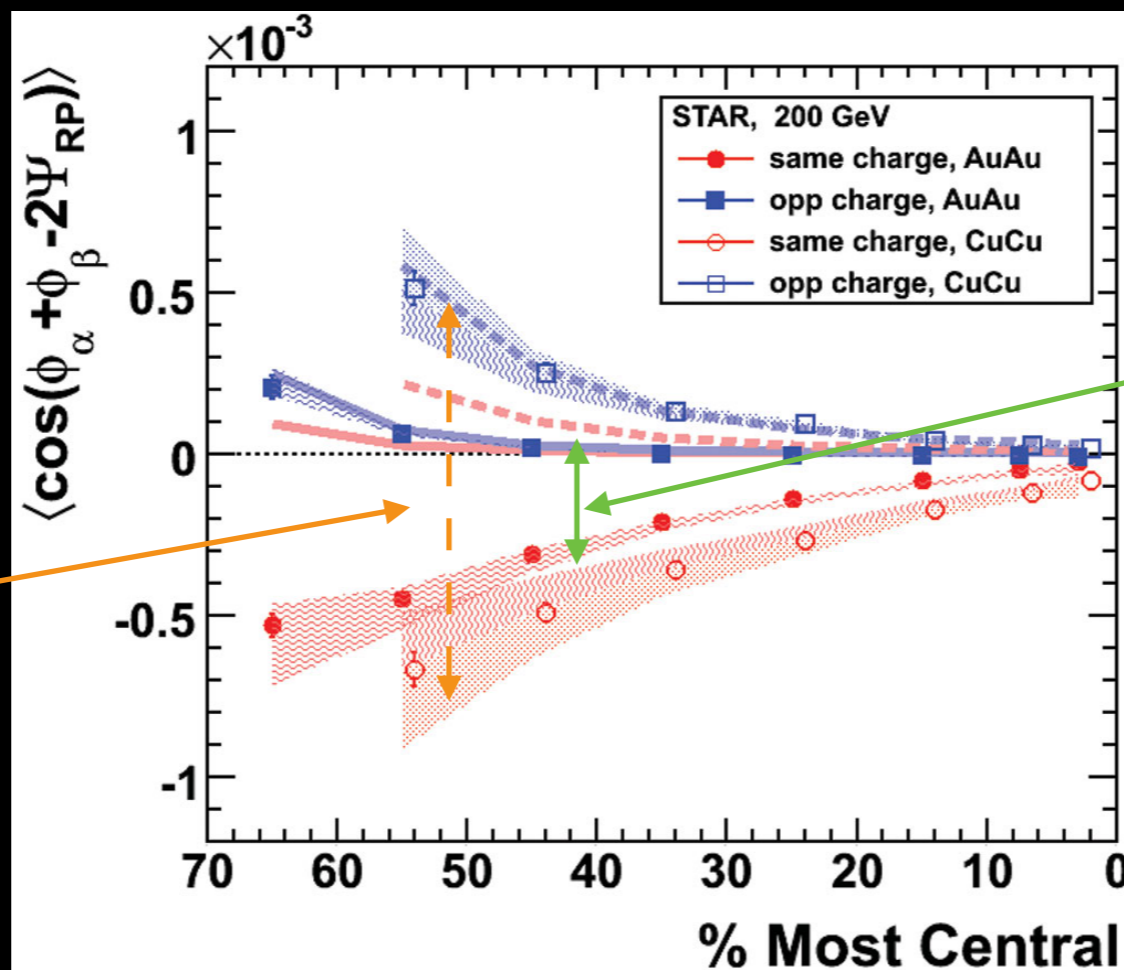
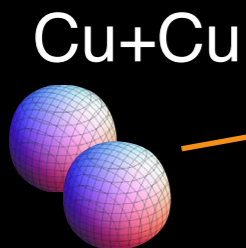
$$\begin{aligned} \gamma^{+-} &= \cos(0 + 0 + 0) = 1 \\ \gamma^{++,--} &= \cos(0 + \pi + 0) = -1 \end{aligned}$$

Voloshin, hep-ph/0406311

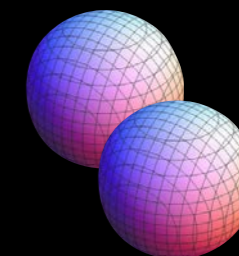
Non-CME effect such as flowing  
resonance decay can lead to difference

$$\Rightarrow \Delta\gamma^{reso} = \gamma^{os} - \gamma^{ss} \propto \frac{v_2^{reso}}{N}$$

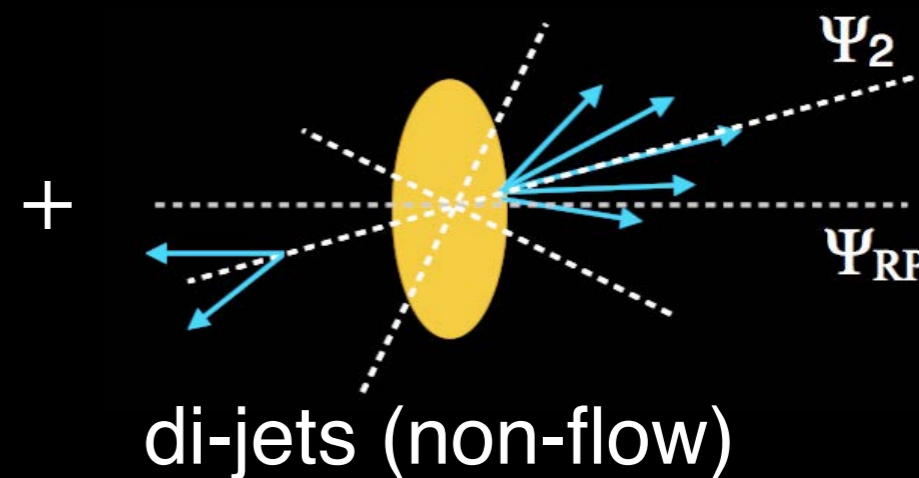
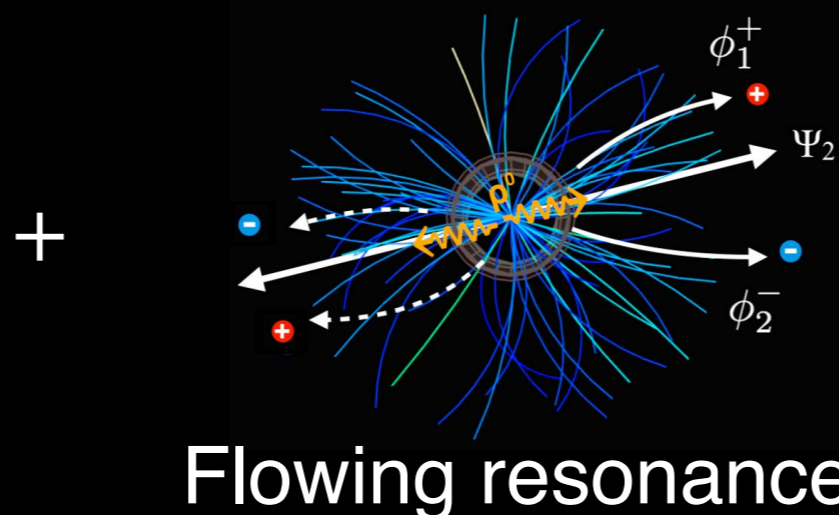
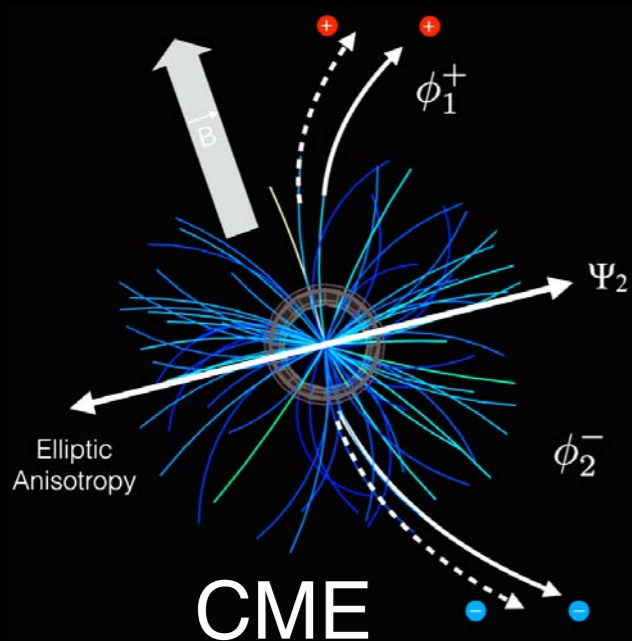
# The first measurements at RHIC



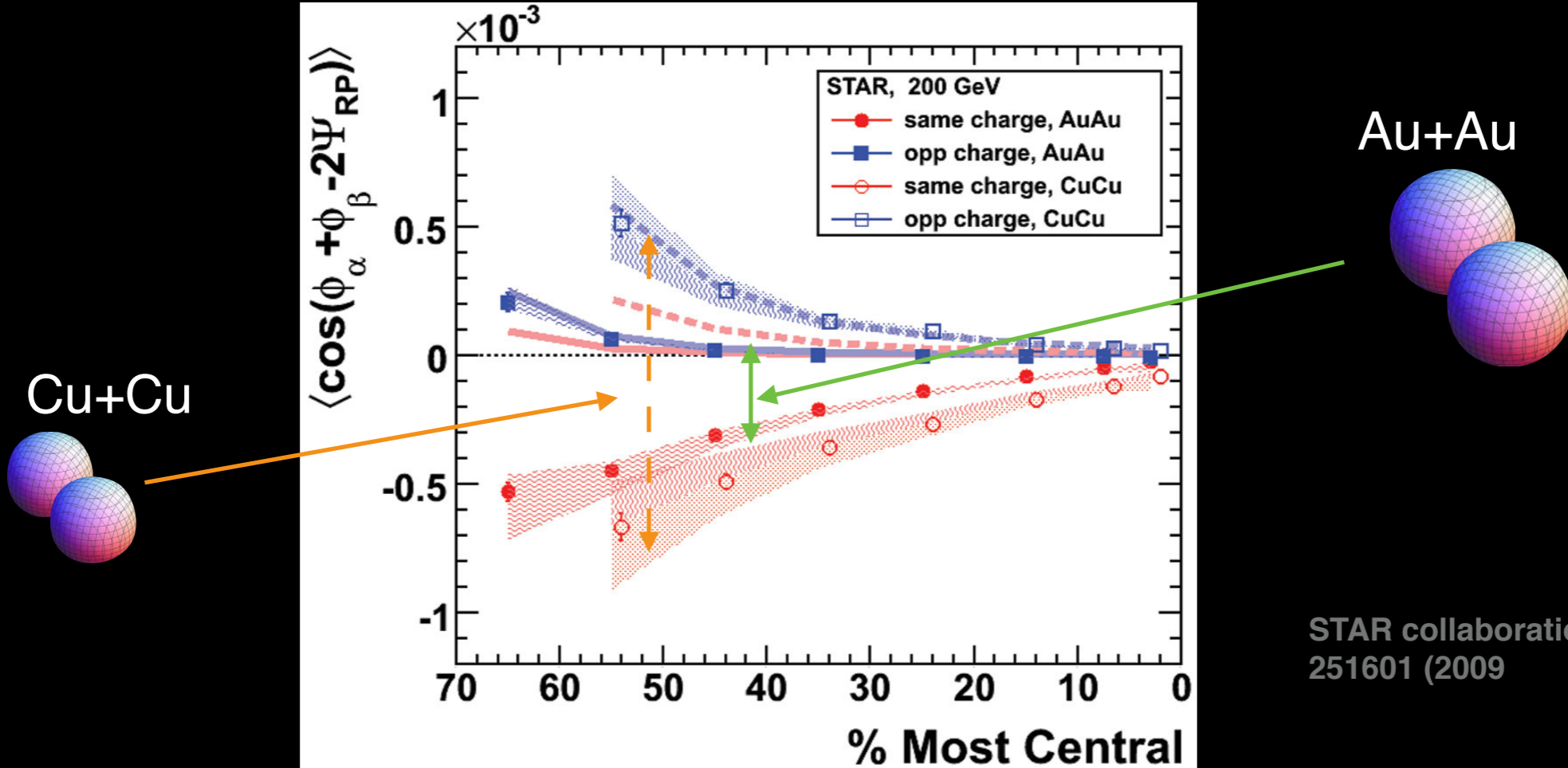
Au+Au



STAR collaboration, PRL 103, 251601 (2009)



# Chirality The first measurements at RHIC



Significant charge separation observed, consistent with CME+ Background

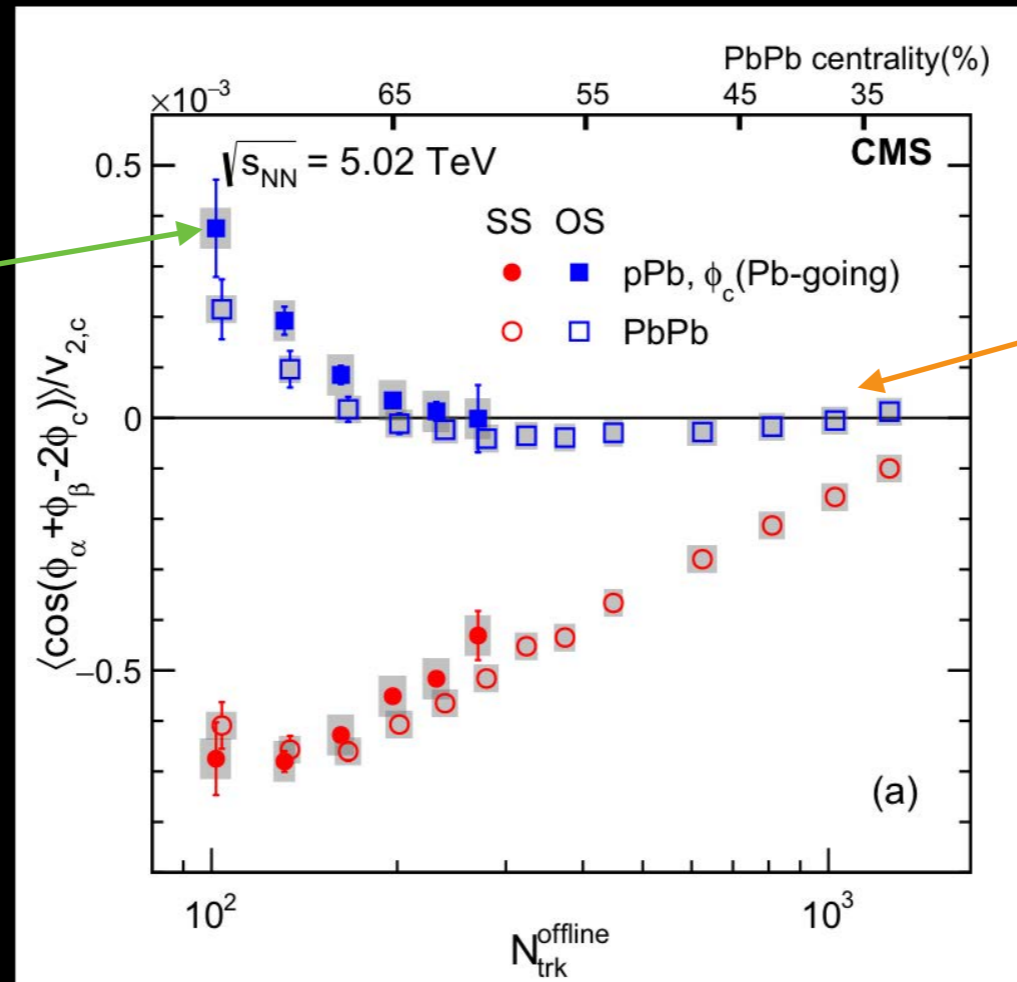
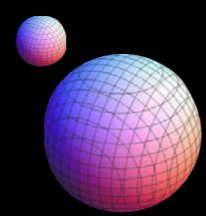
$$\Delta\gamma = \Delta\gamma^{CME} + k \times \frac{v_2}{N} + \Delta\gamma^{non-flow}$$

Measurement      Signal      Background-1      Background-2

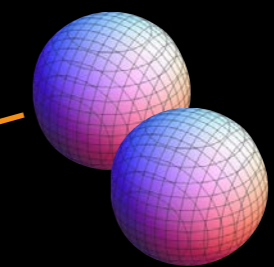


# Small system collisions to test CME

p+A



A+A



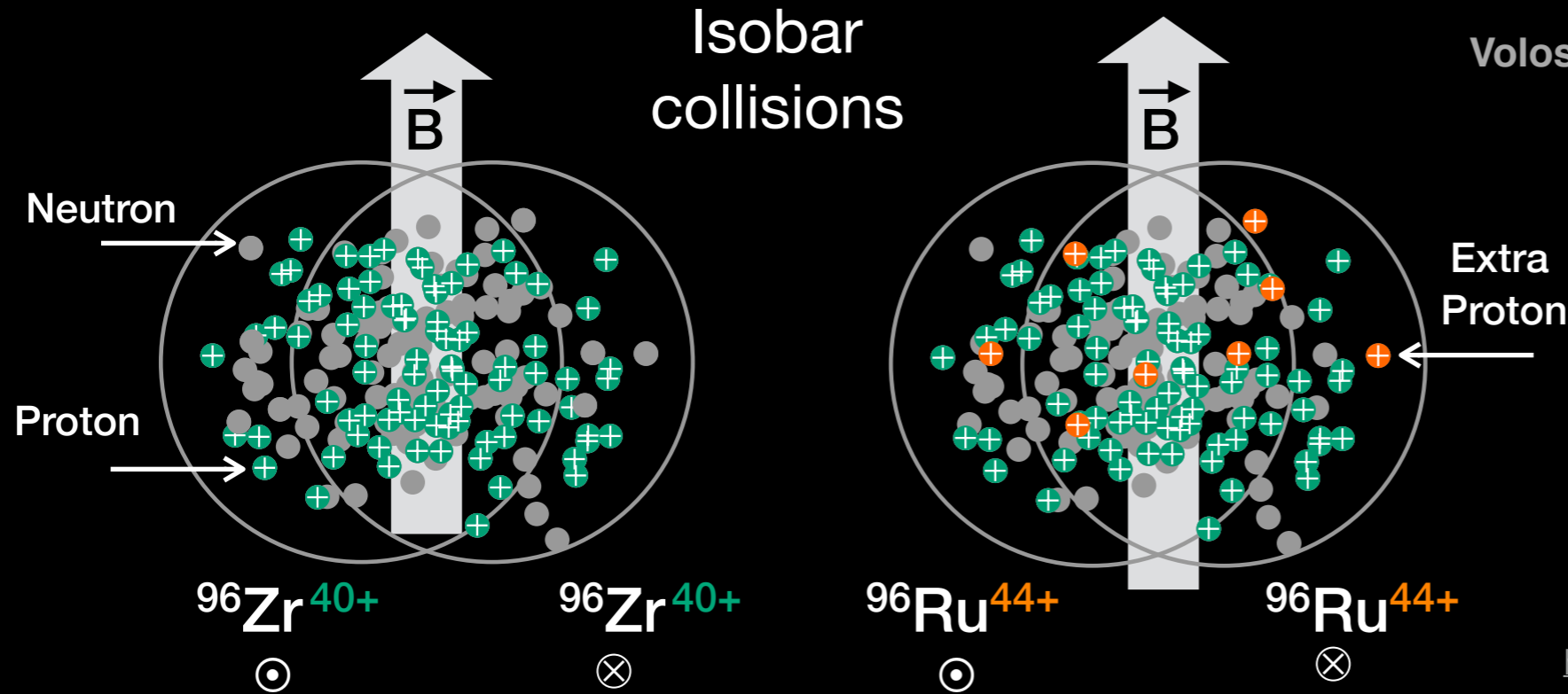
CMS collaboration, Phys. Rev Lett, 118 (2017) 122301

$$\left\{ \begin{array}{l}
 \Delta\gamma^{A+A} = \Delta\gamma^{CME} + k \times \frac{v_2}{N} + \Delta\gamma^{non-flow} \\
 \parallel \quad \quad \quad \neq \quad \quad \quad \neq \quad \quad \quad \neq \\
 \Delta\gamma^{p+A} = \cancel{\Delta\gamma^{CME}} + k \times \frac{v_2}{N} + \Delta\gamma^{non-flow}
 \end{array} \right.$$

Only two equations & more unknowns difficult to prove if  $\Delta\gamma^{CME} = 0$

Two systems of very different sizes → limited control over background (This naturally leads to the idea of using two systems of similar sizes)

# Isobar collisions



Voloshin, Phys.Rev.Lett. 105 (2010) 172301

Isobar collisions provide the best possible control of signal and background compared to all previous experiments

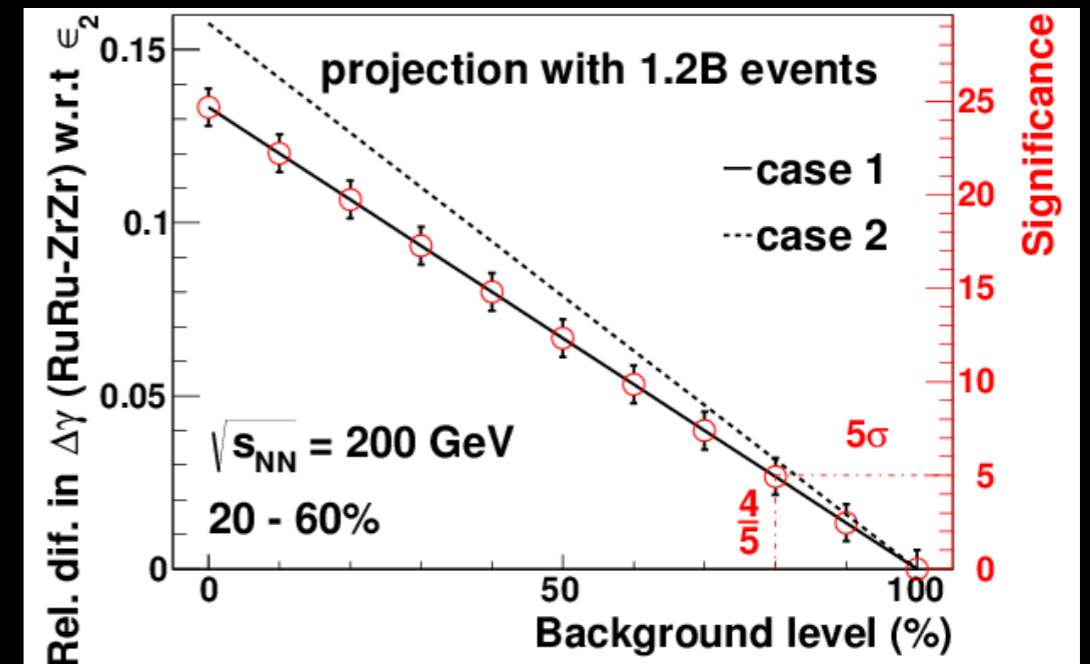
[https://drupal.star.bnl.gov/STAR/system/files/STAR\\_BUR\\_Run1718\\_v22\\_0.pdf](https://drupal.star.bnl.gov/STAR/system/files/STAR_BUR_Run1718_v22_0.pdf)

$$\Delta\gamma^{\text{Ru+Ru}} = \Delta\gamma^{\text{CME}} + k \times \frac{v_2}{N} + \Delta\gamma^{\text{non-flow}}$$

?? † ‡ ||

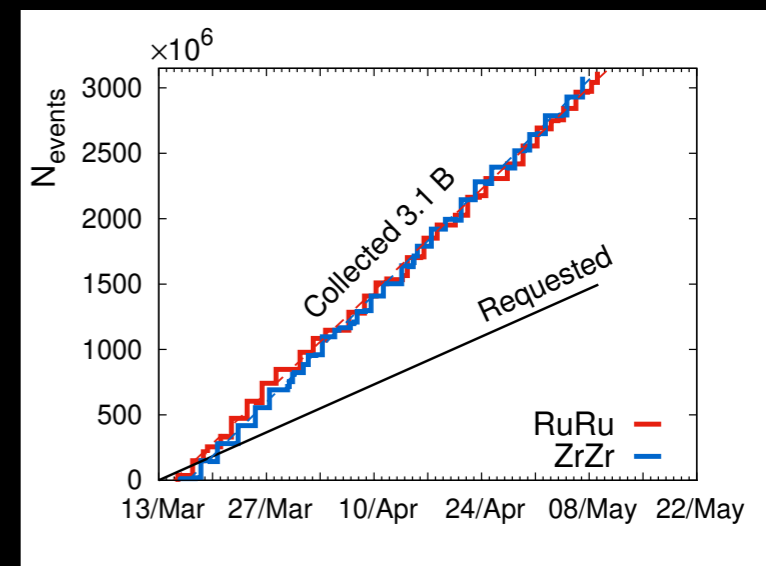
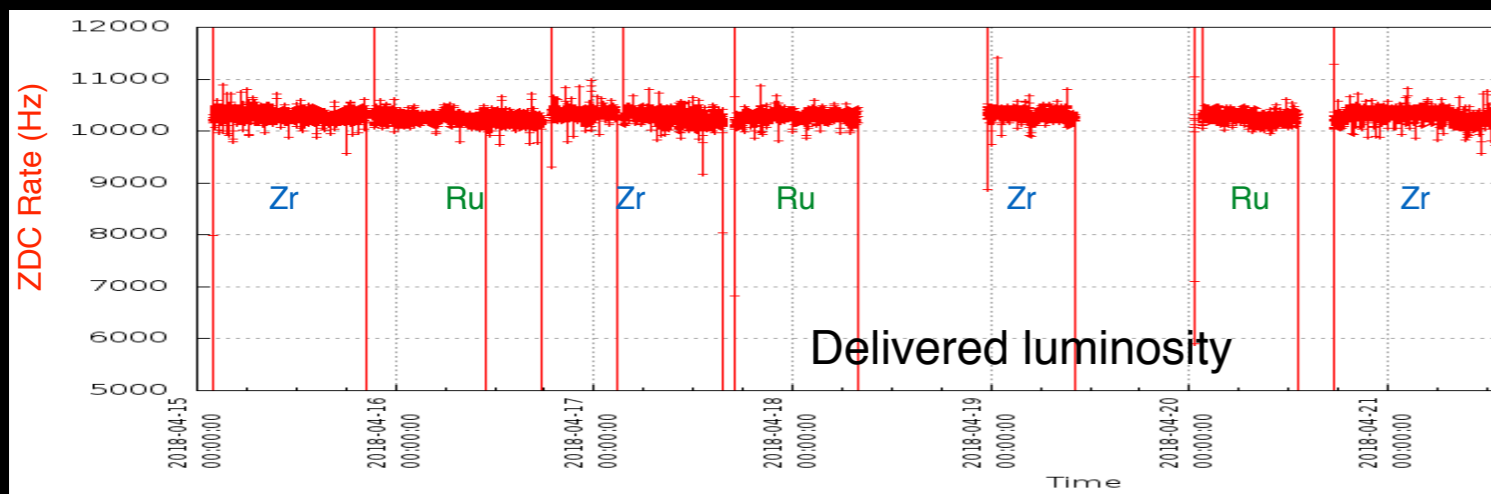
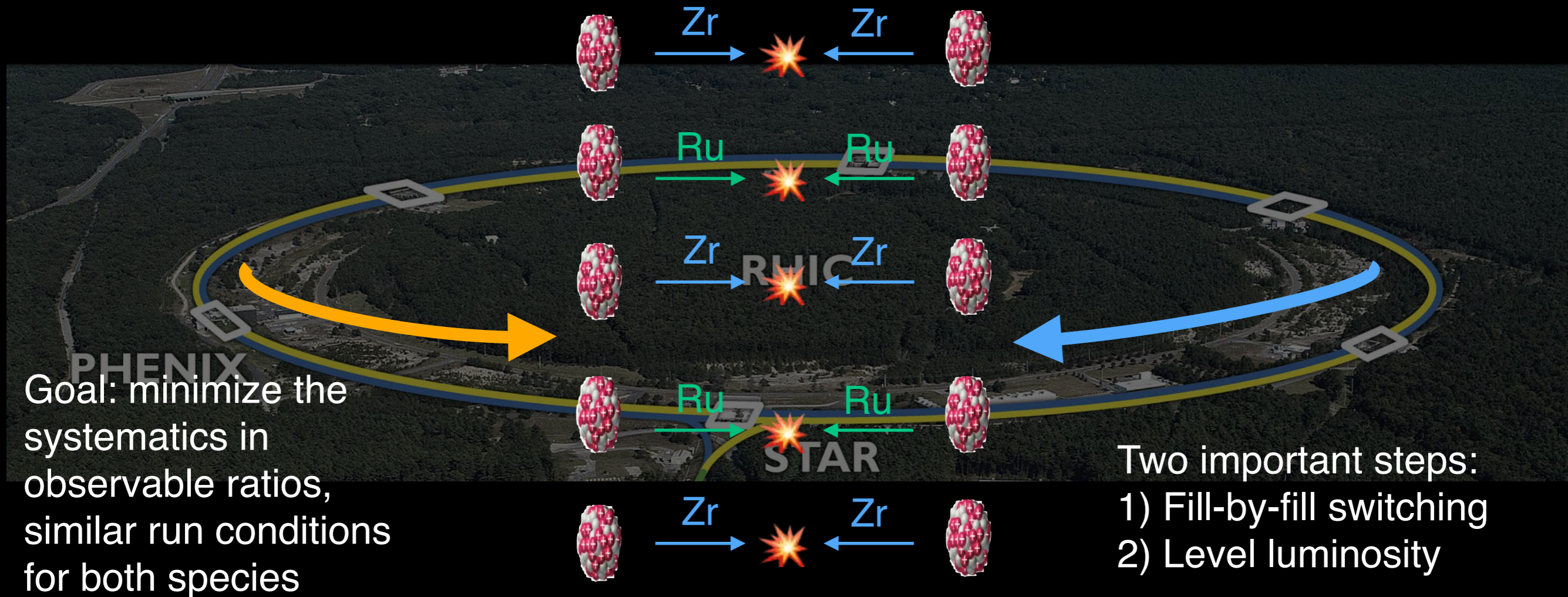
$$\Delta\gamma^{\text{Zr+Zr}} = \Delta\gamma^{\text{CME}} + k \times \frac{v_2}{N} + \Delta\gamma^{\text{non-flow}}$$

B-field 10-18% larger in Ru      Within 0-4%      Same



Larger signal in Ru: 1.2 B events can give  $5\sigma$  significance for 20% signal level

# Details Of The Data Taking Of The Isobar Run

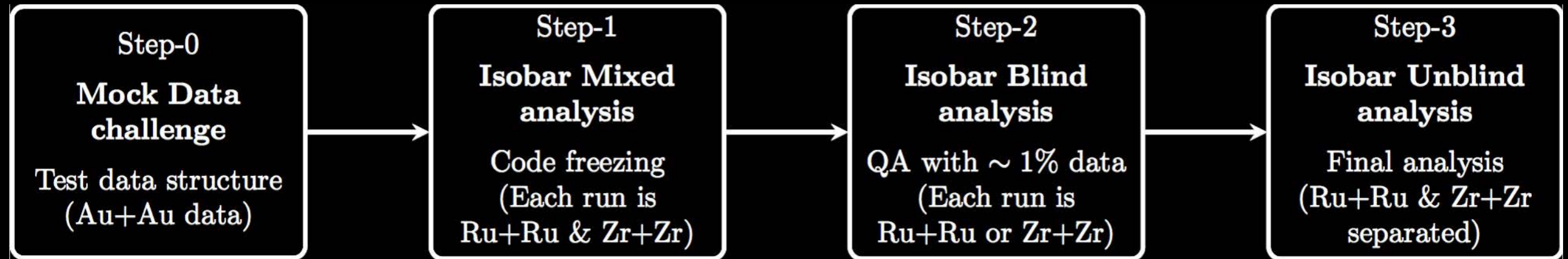


G. Marr et al., in 10th International Particle Accelerator Conference (2019) pp. 28–32.

# Blind analysis of the isobar data



# Steps of Isobar blind analysis



NPP PAC recommended a blind analysis of isobar data

Blinding committee decides the procedure

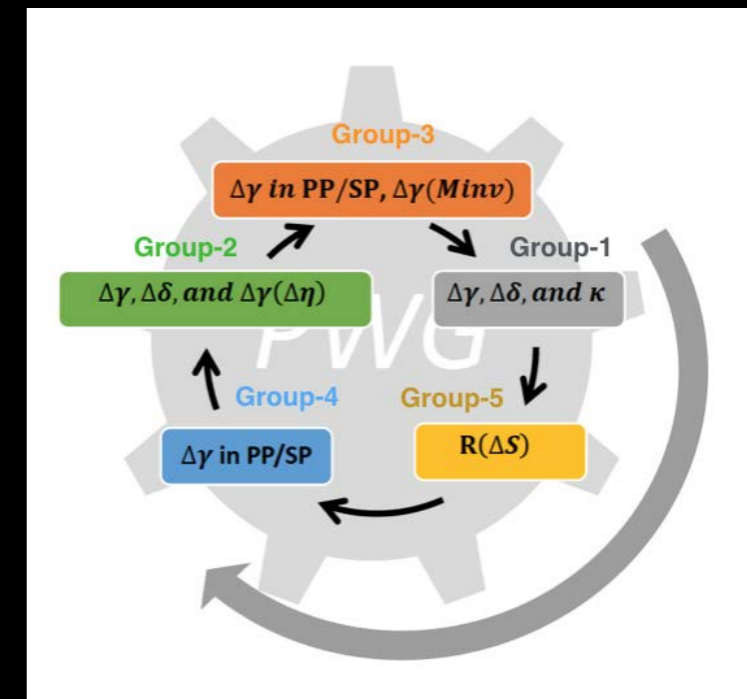
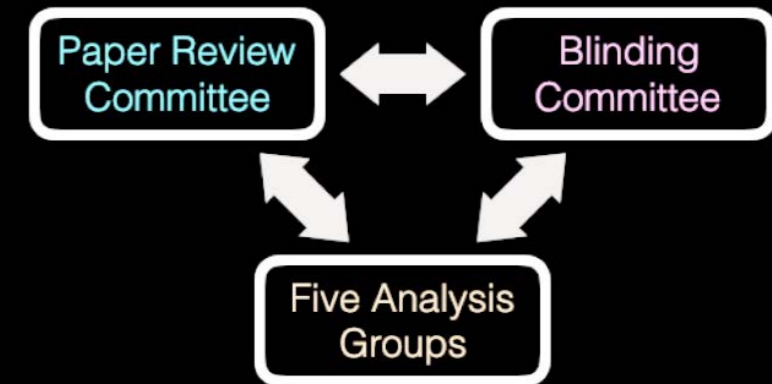
Five independent groups will perform analysis

No access to species-specific information before last step

Everything documented (not written → not allowed)

Case for CME & interpretation must be pre-defined

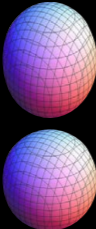
All codes must be frozen and run by another person



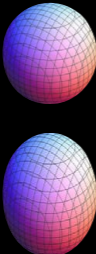
# Centrality determination

Blind analysis: we decided to compare observables at same centralities between isobars

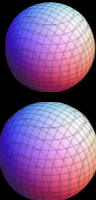
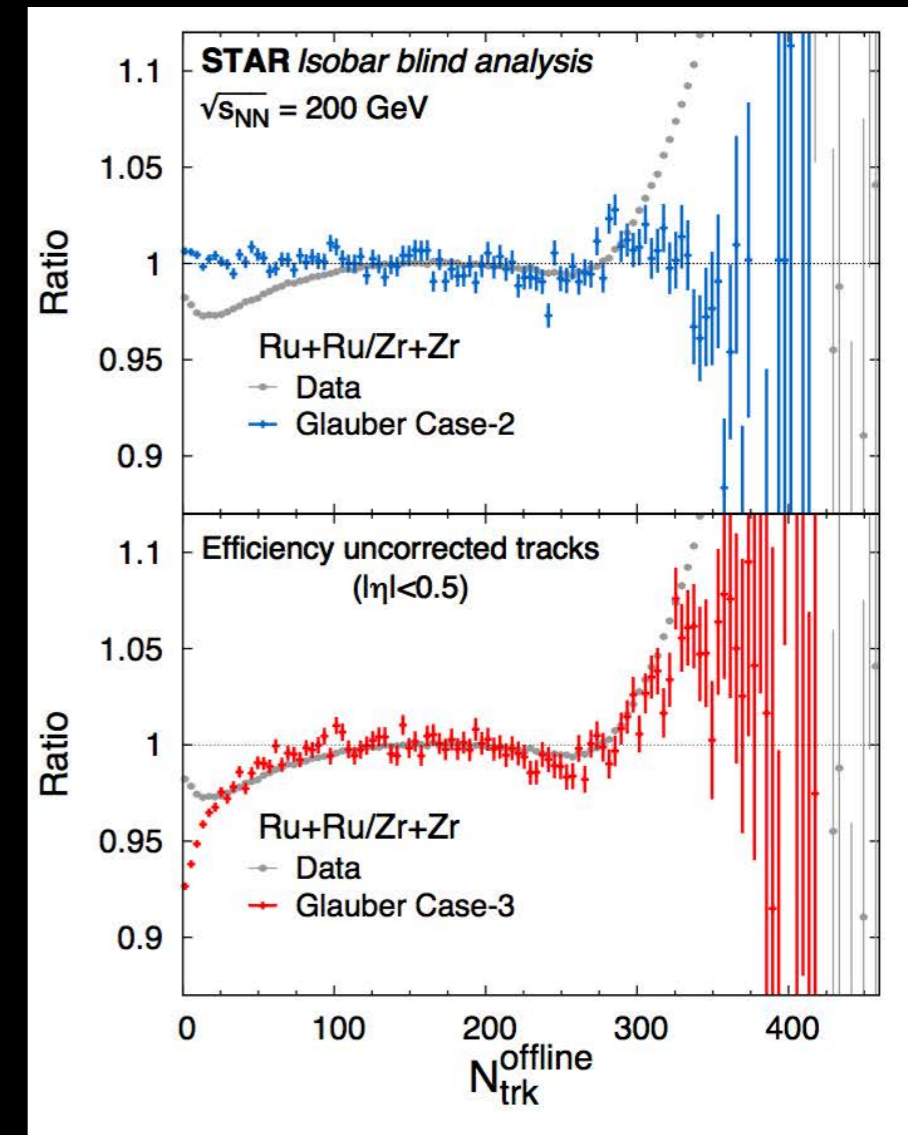
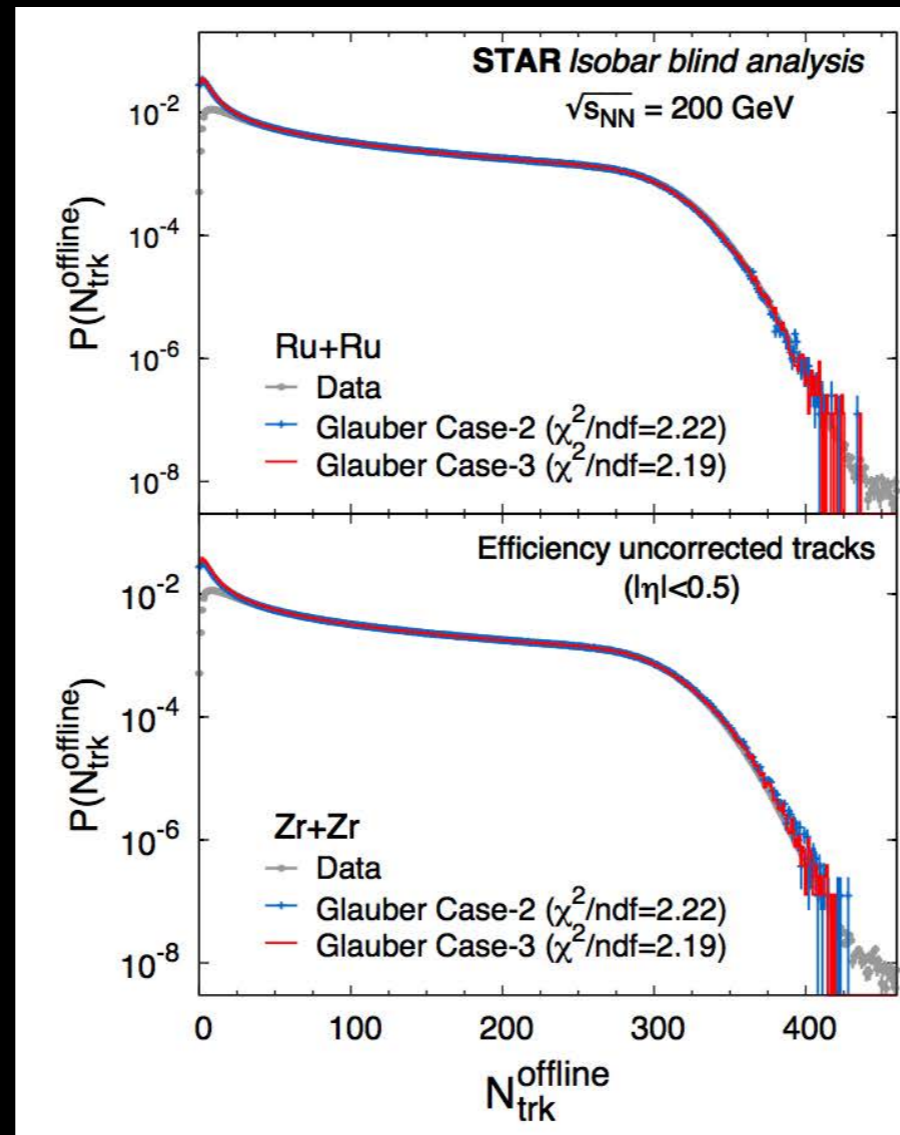
Case-1 [83]			
Nucleus	$R$ (fm)	$a$ (fm)	$\beta_2$
$^{96}_{44}\text{Ru}$	5.085	0.46	0.158
$^{96}_{40}\text{Zr}$	5.02	0.46	0.08



Case-2 [83]			
Nucleus	$R$ (fm)	$a$ (fm)	$\beta_2$
$^{96}_{44}\text{Ru}$	5.085	0.46	0.053
$^{96}_{40}\text{Zr}$	5.02	0.46	0.217



Case-3 [113]			
Nucleus	$R$ (fm)	$a$ (fm)	$\beta_2$
$^{96}_{44}\text{Ru}$	5.067	0.500	0
$^{96}_{40}\text{Zr}$	4.965	0.556	0

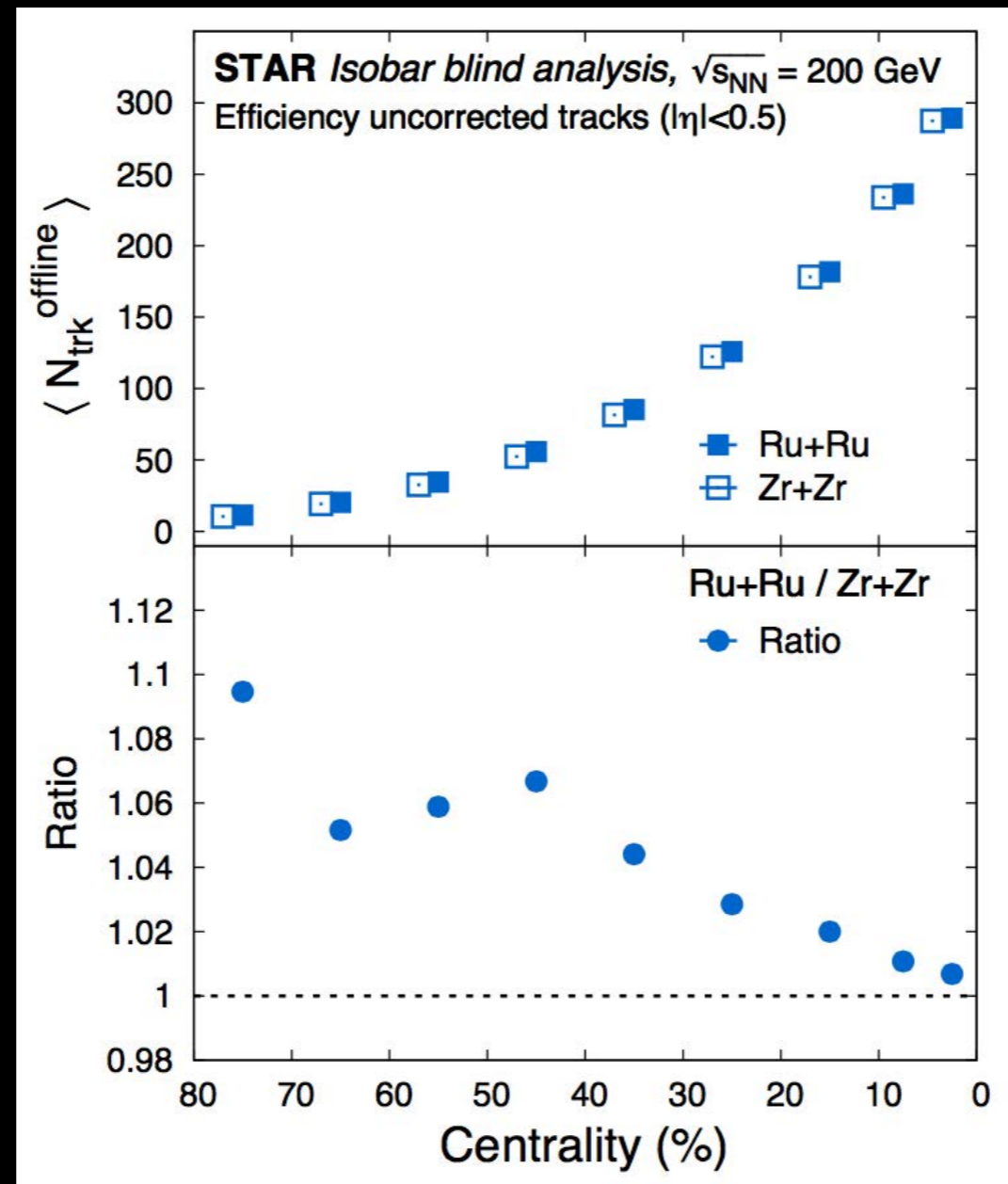
See references in:

[83] Deng et. al., Phys. Rev. C 94, 041901 (2016), arXiv:1607.04697 [nucl-th].

[113] Xu et. al., Phys. Rev. Lett. 121, 022301 (2018), arXiv:1710.03086 [nucl-th].

MC-Glauber with two-component model used to describe uncorrected multiplicity distribution. WS parameters with no deformation (thicker neutron skin in Zr) provides the best description of the multiplicity distributions

# Multiplicity difference between the isobars

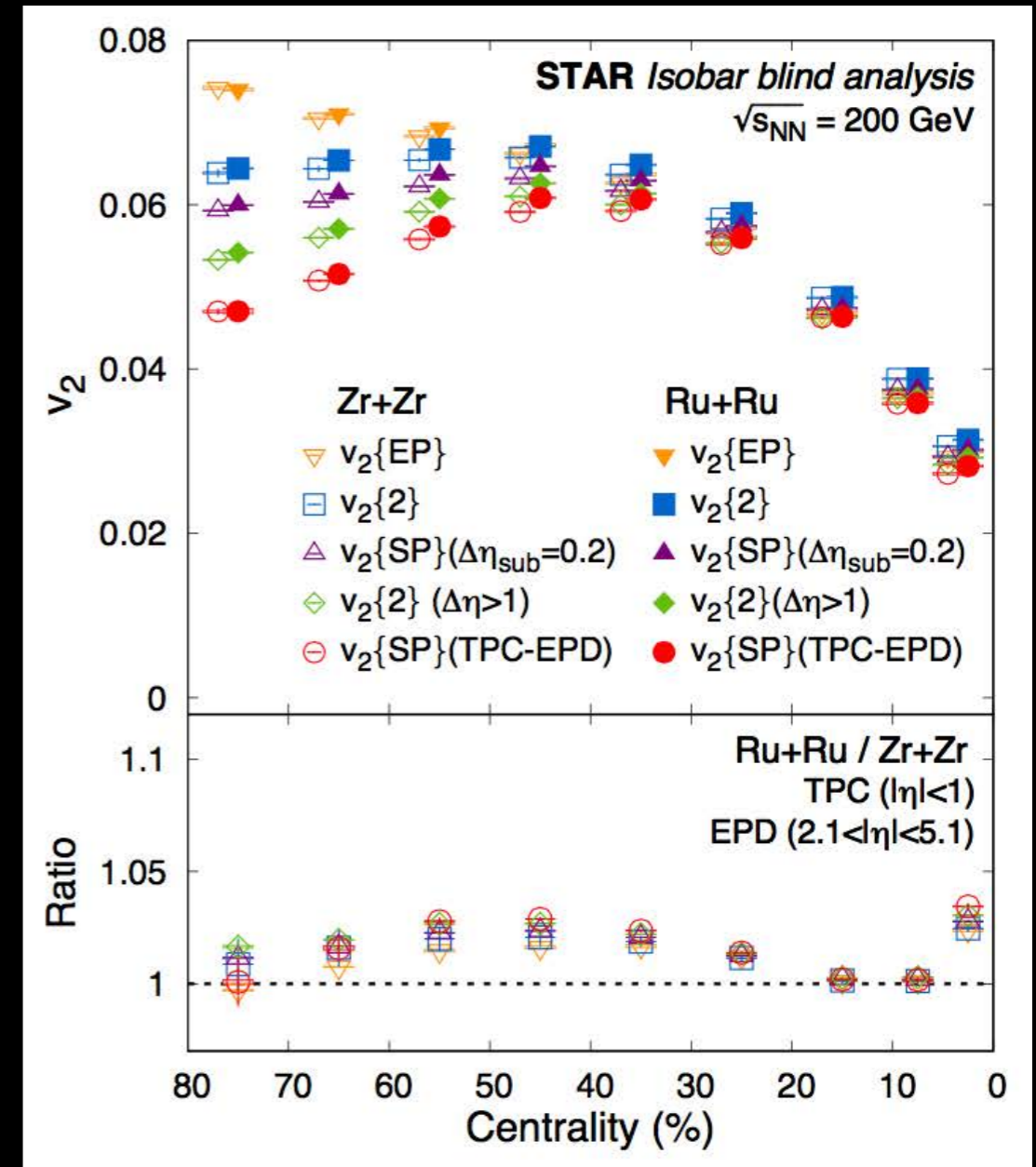
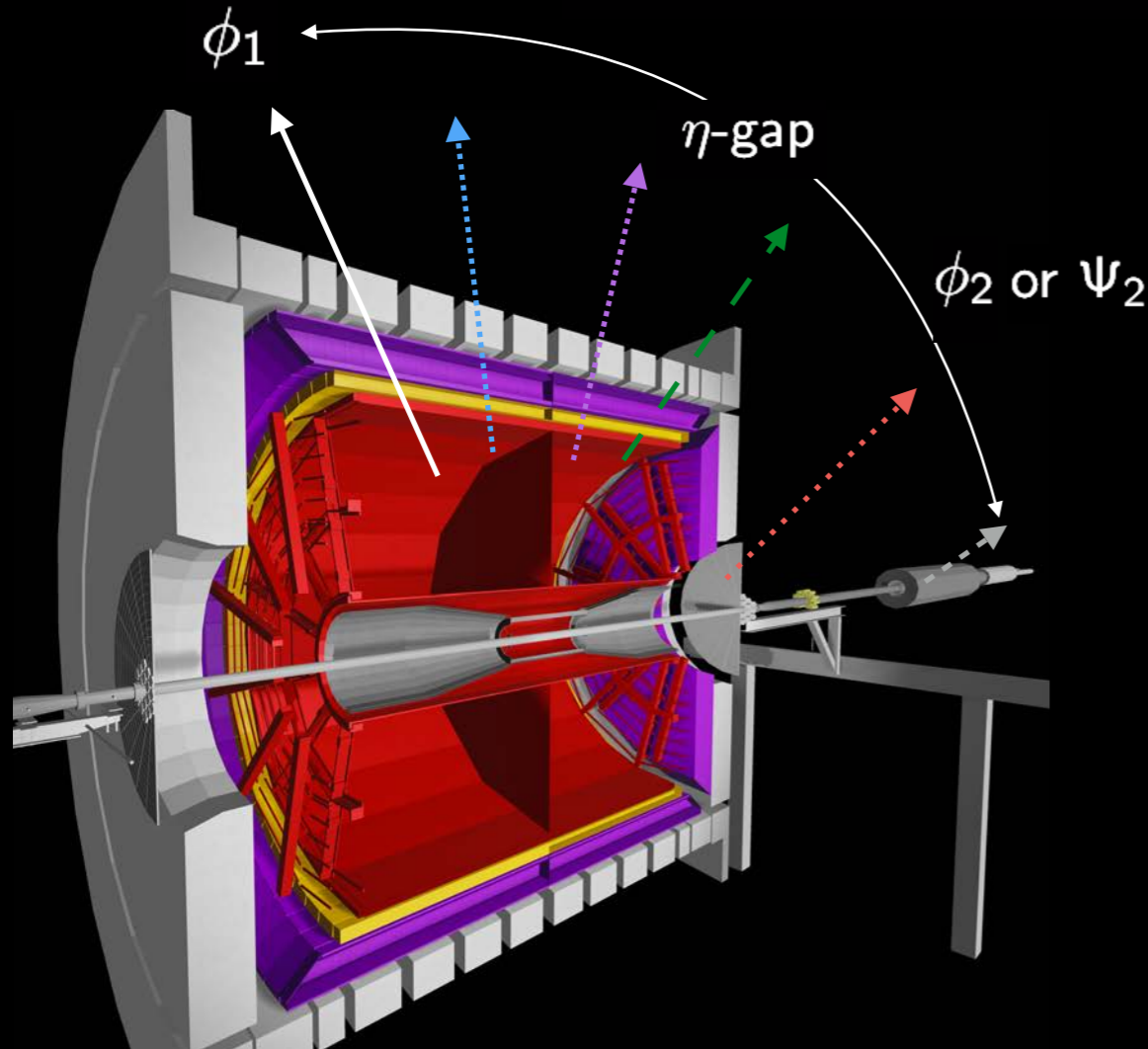


Mean efficiency uncorrected multiplicity density is larger in Ru than in Zr in a matching centrality, this can affect signal and background difference between isobars

# Elliptic flow difference between the isobars

$$v_2\{EP\} = \langle \cos(2\phi_1 - 2\Psi_2) \rangle$$

$$v_2\{2\}^2 = \langle \cos(2\phi_1 - 2\phi_2) \rangle$$



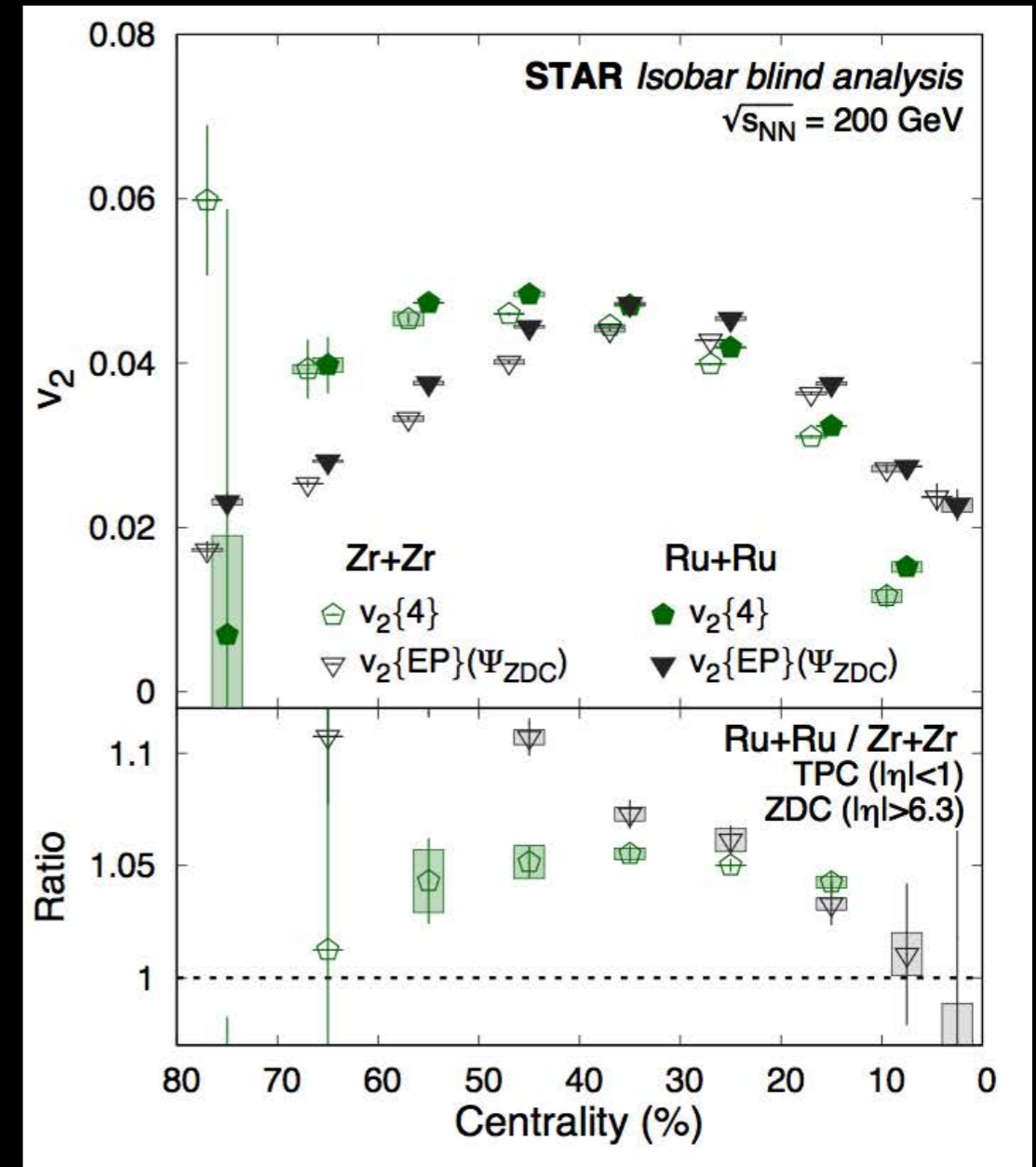
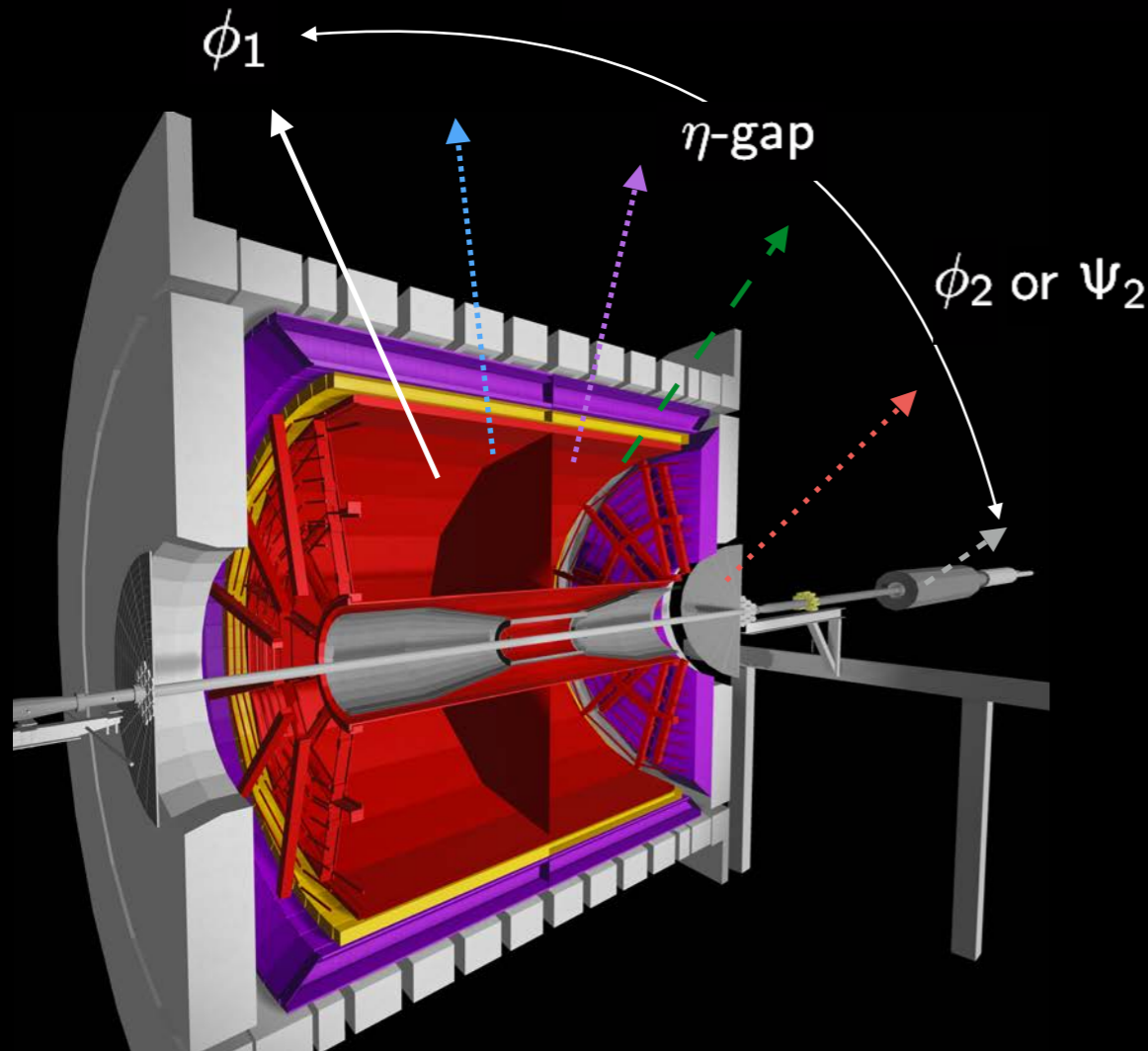
$v_2$  studied  $\eta$ -gap (including EPDs), ratio deviates from unity indicating difference in the shape, nuclear structure between two isobars (larger quadrupole deformation in Ru+Ru)



# Elliptic flow difference between isobars

$$v_2\{EP\} = \langle \cos(2\phi_1 - 2\Psi_2) \rangle$$

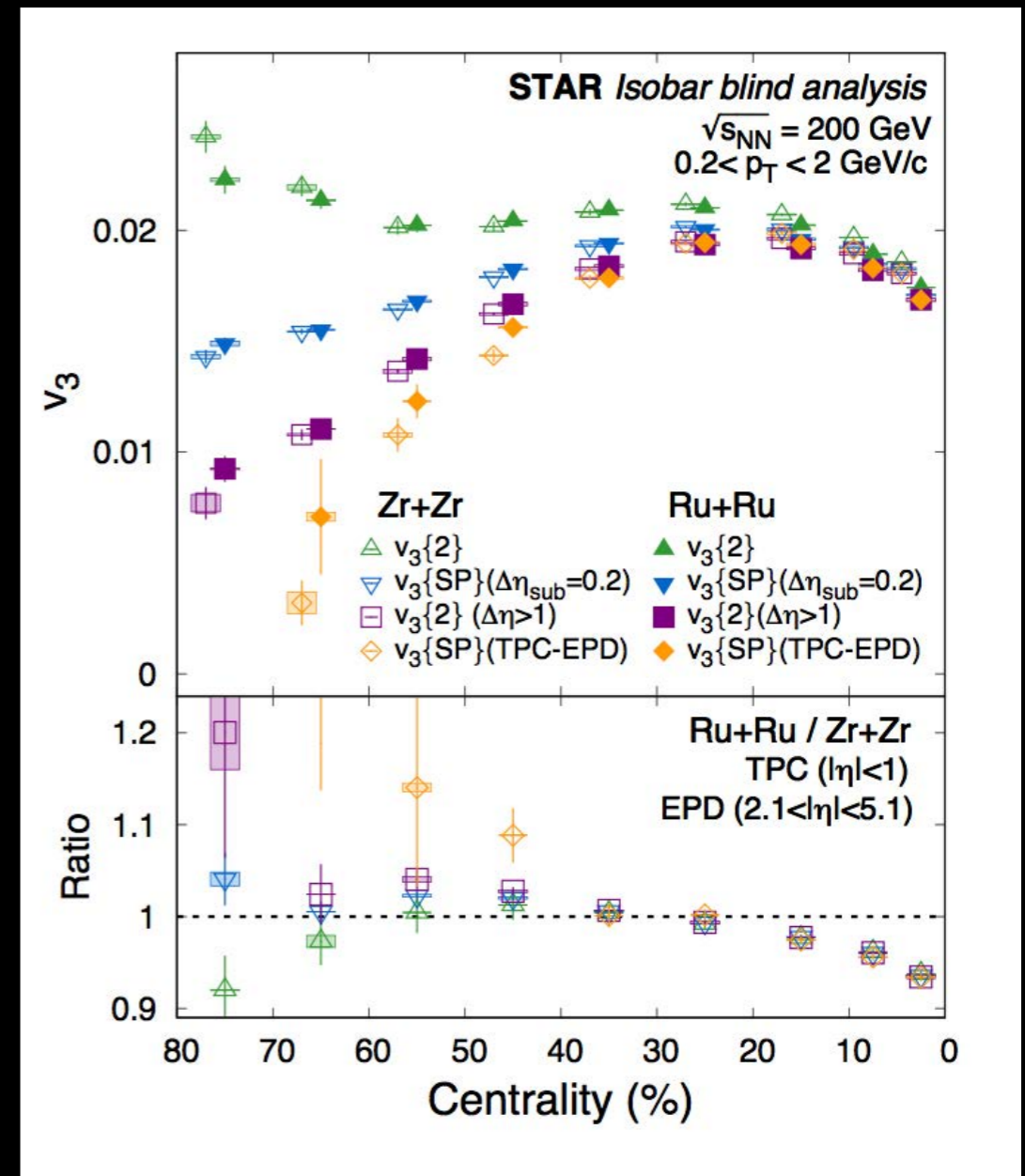
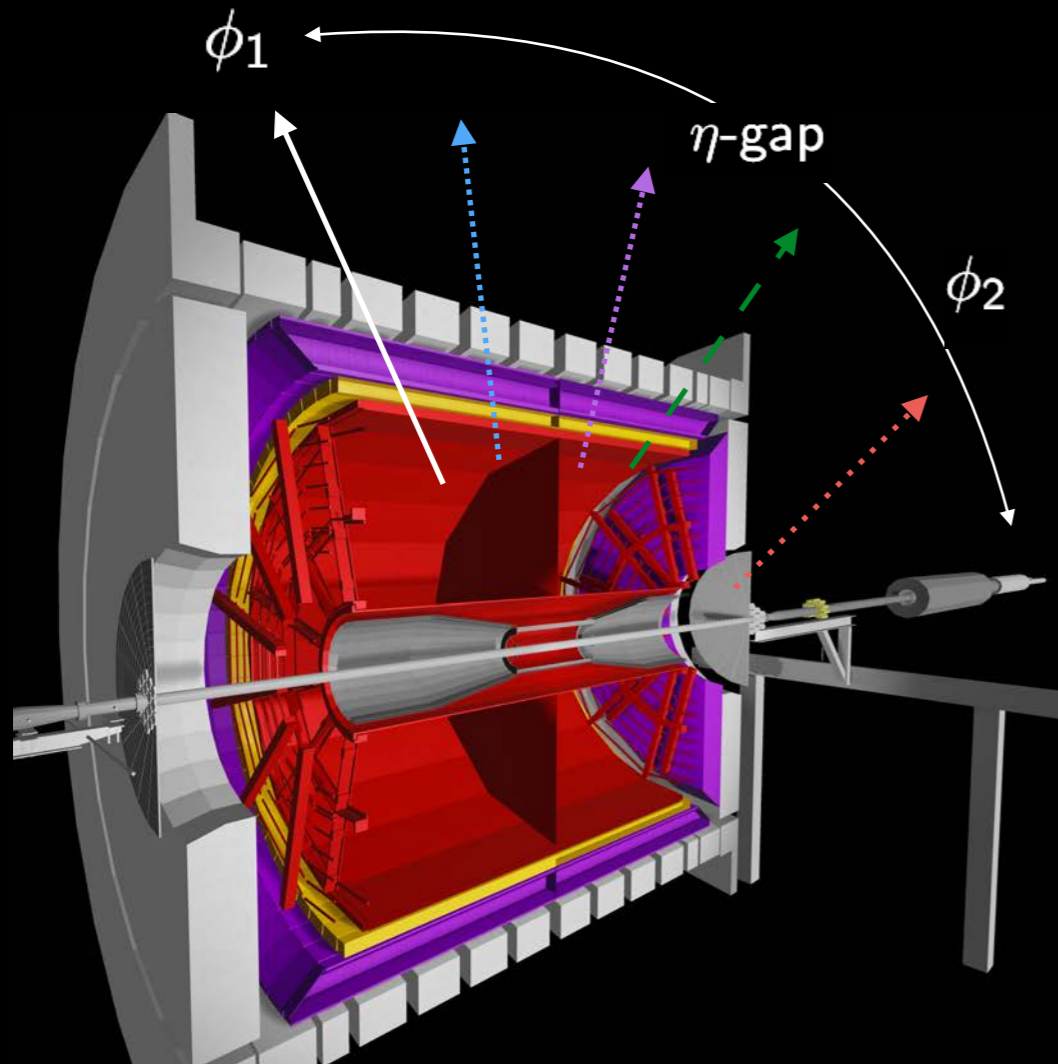
$$v_2\{2\}^2 = \langle \cos(2\phi_1 - 2\phi_2) \rangle$$



$v_2$  studied  $\eta$ -gap (including EPDs), ratio deviates from unity indicating difference in the shape, nuclear structure between two isobars (larger quadruple deformation in Ru+Ru)

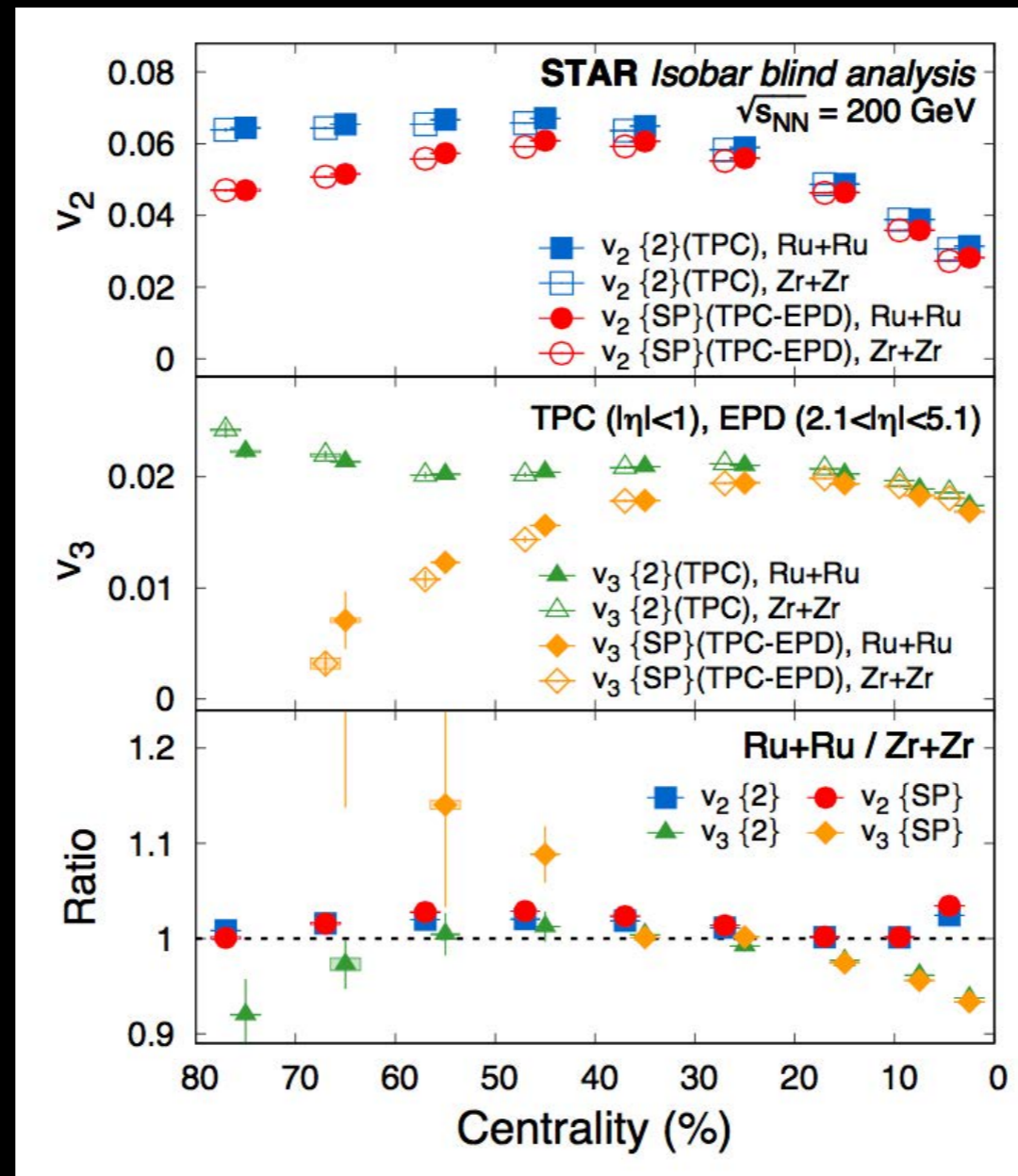
# Triangular flow difference between isobars

$$v_3\{2\}^2 = \langle \cos(3\phi_1 - 3\phi_2) \rangle$$



Strong rapidity dependence, ratio below unity in central collisions, not fully understood

# v2 and v3 comparison for the isobars

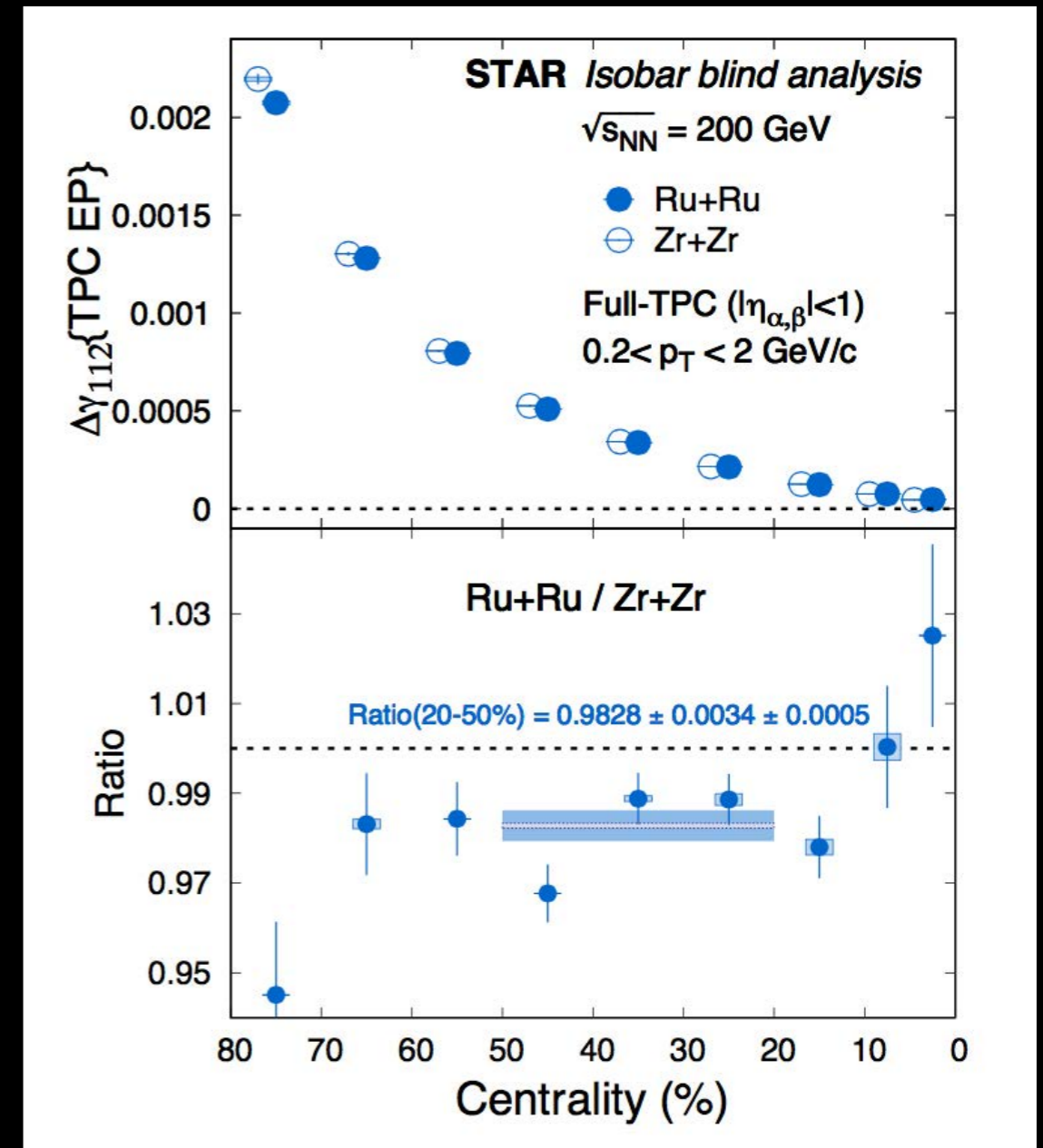
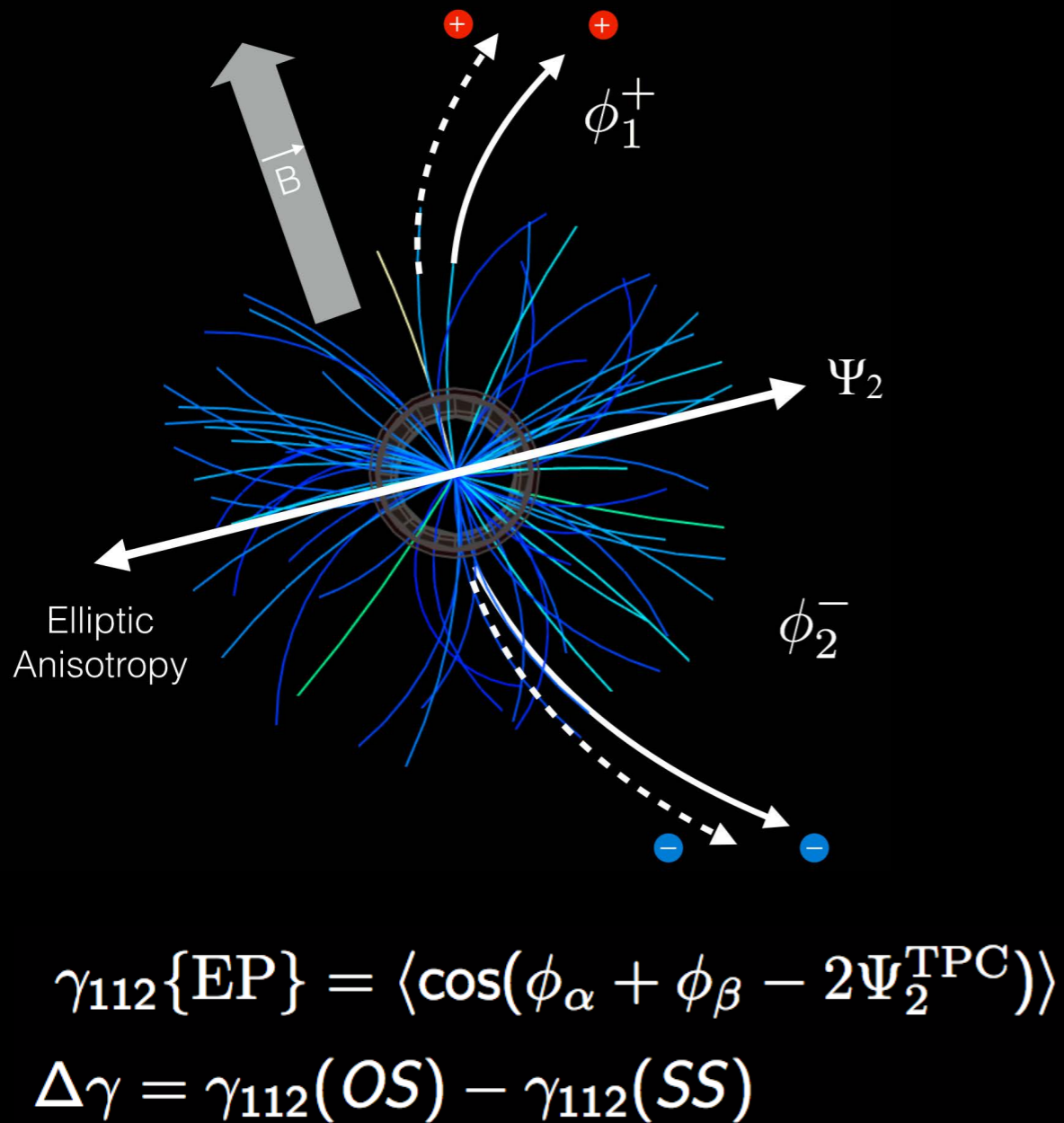


$v_n$  ratio deviates from unity indicating difference in the shape, nuclear structure between two isobars.  $v_n$  drives flow-driven background:

$$\Delta\gamma^{bkg} = \gamma^{OS} - \gamma^{SS} \propto \frac{v_2^{reso}}{N}$$

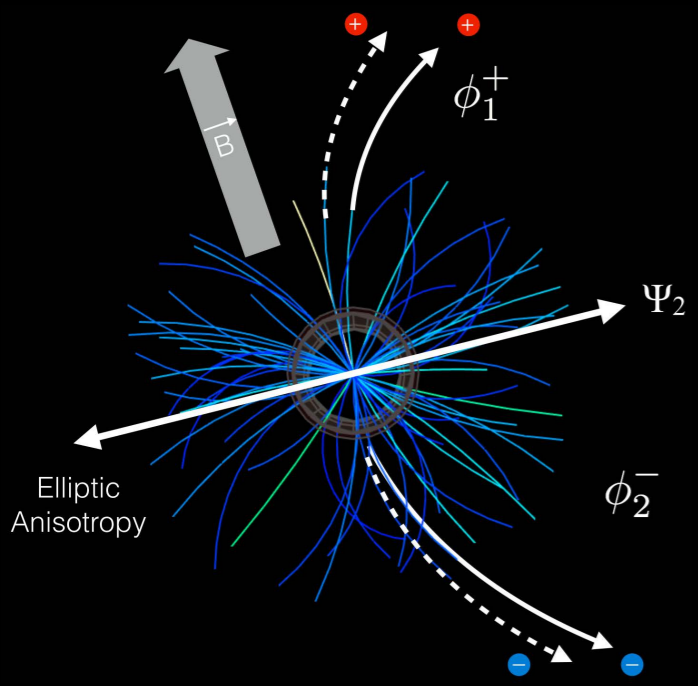
# Results on CME sensitive variables

# Charge separation across elliptic flow plane



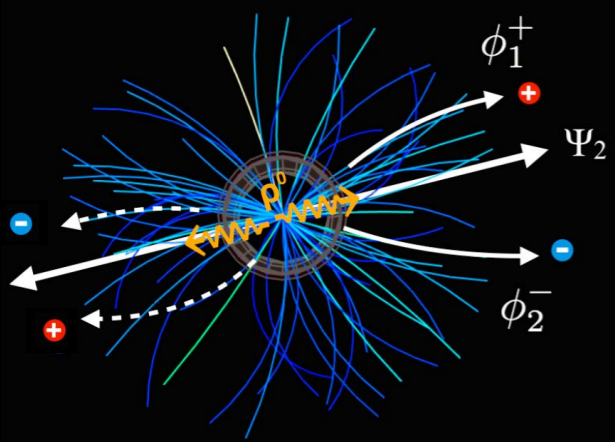
Ratio of charge separation correlated to elliptic flow plane is below unity, however only this quantity is not decisive

# Charge separation scaled by elliptic flow



$$\gamma_{112}\{\text{EP}\} = \langle \cos(\phi_\alpha + \phi_\beta - 2\Psi_2^{\text{TPC}}) \rangle$$

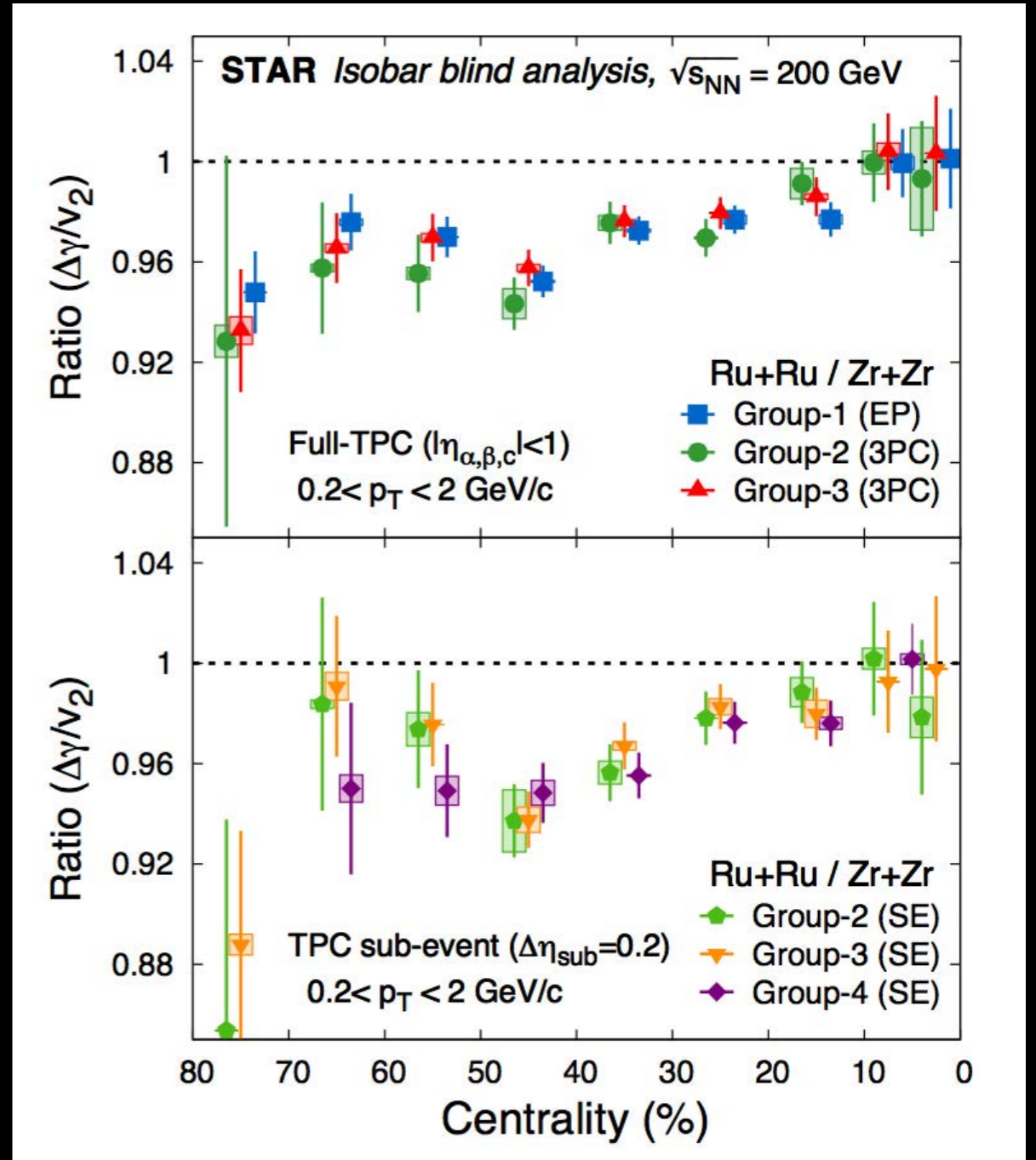
$$\Delta\gamma = \gamma_{112}(\text{OS}) - \gamma_{112}(\text{SS})$$



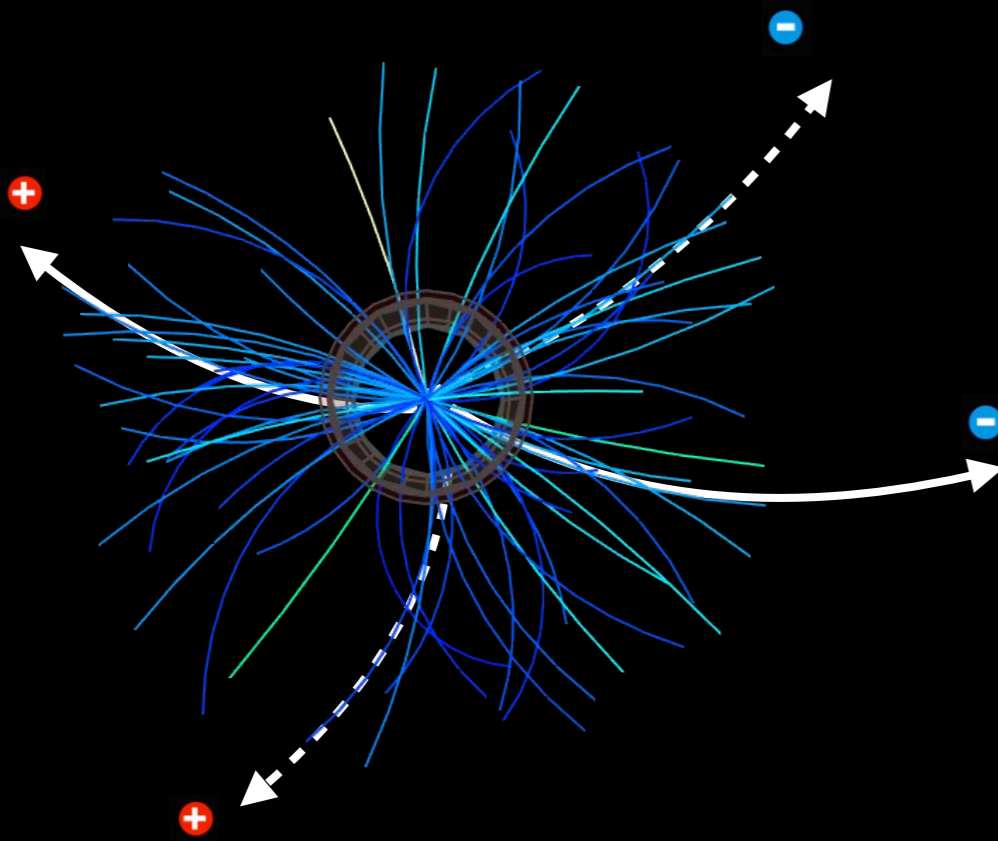
$$\Delta\gamma^{bkg} = \gamma^{OS} - \gamma^{SS} \propto \frac{v_2^{reso}}{N}$$

Pre-defined criteria for CME

$$\frac{(\Delta\gamma/v_2)_{\text{RuRu}}}{(\Delta\gamma/v_2)_{\text{ZrZr}}} > 1 \quad \text{NOT seen}$$

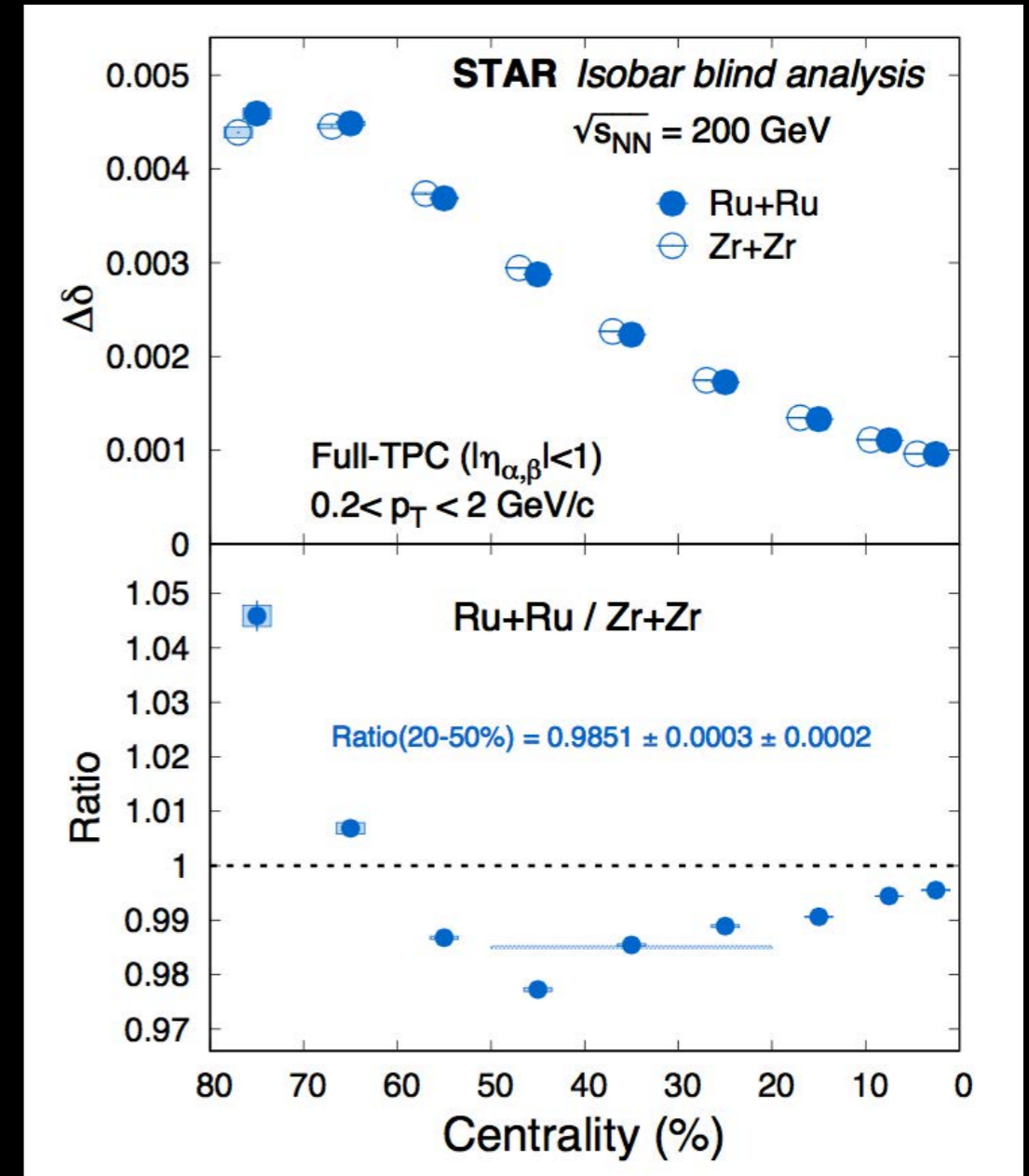


# Two-particle correlator of charge separation



$$\delta \equiv \langle \cos(\phi_\alpha - \phi_\beta) \rangle$$

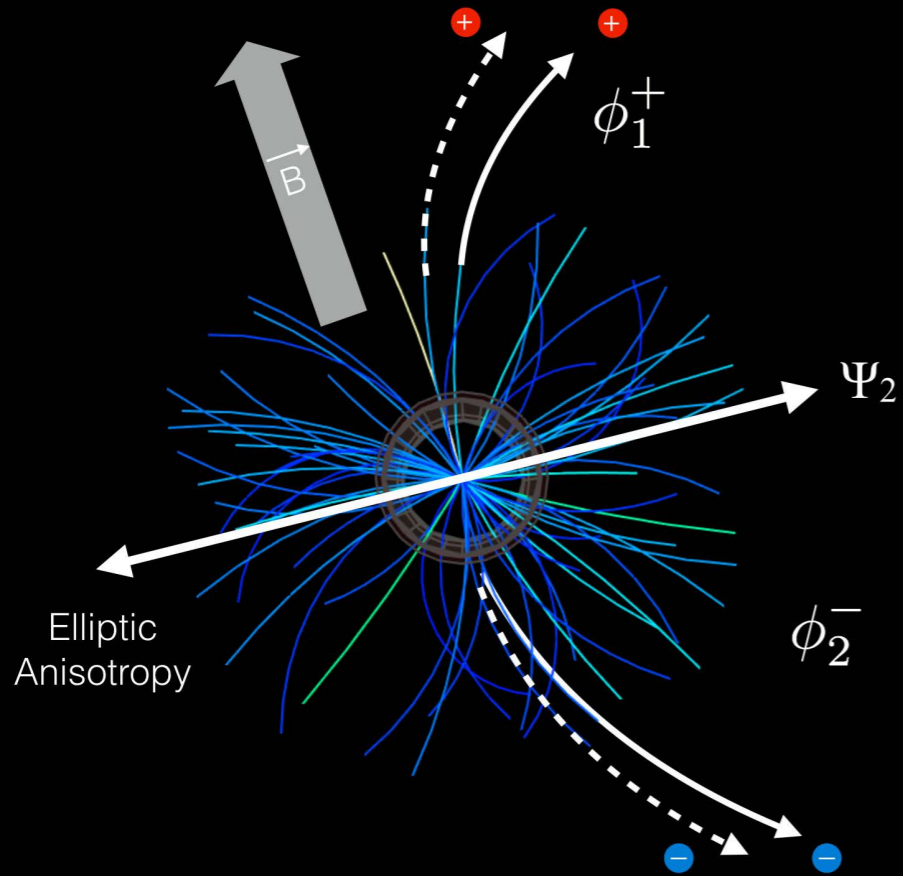
$$\Delta\delta = \delta(OS) - \delta(SS)$$



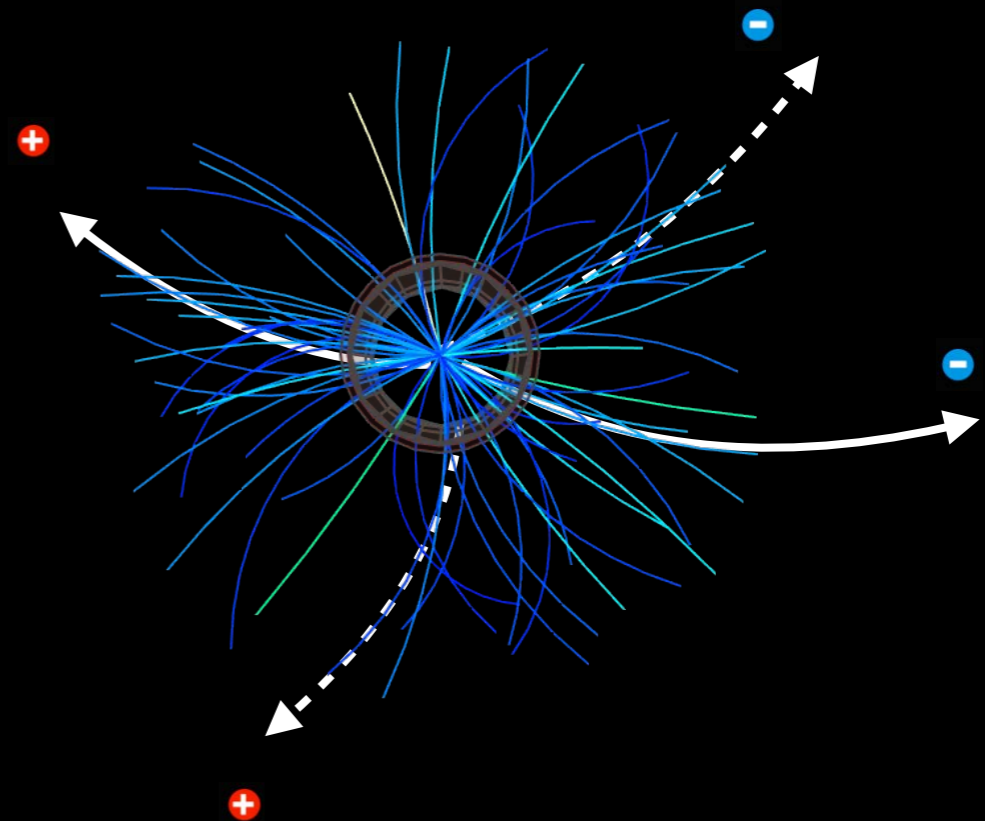
Two particle-charge separation observable  $\delta$ -correlator — measures charge separation that may or may not be correlated to event plane.

# Charge separation across elliptic flow plane

Charge separation correlated to event plane



Charge dependent two-particle correlation



$$\begin{aligned} \gamma_{112}\{\text{EP}\} &= \langle \cos(\phi_\alpha + \phi_\beta - 2\Psi_2^{\text{TPC}}) \rangle \\ &= \langle \cos(\phi_\alpha - \phi_\beta + 2\phi_\beta - 2\Psi_2) \rangle \\ &\approx \langle \cos(\phi_\alpha - \phi_\beta) \cos(2\phi_\beta - 2\Psi_2) \rangle \\ &= \kappa_{112} \langle \cos(\phi_\alpha - \phi_\beta) \rangle \langle \cos(2\phi_\beta - 2\Psi_2) \rangle \end{aligned}$$

$\Leftrightarrow$

$$\begin{aligned} \delta &= \langle \cos(\phi_\alpha - \phi_\beta) \rangle \\ &\times \\ v_2 &= \langle \cos(2\phi - \Psi_2) \rangle \end{aligned}$$

$$\gamma_{112} \equiv \kappa_{112} \delta v_2$$

This factorization breaking coefficient should be  $>1$  and can help test CME



# Ratio of factorization breaking

$$\gamma_{112}\{\text{EP}\} = \langle \cos(\phi_\alpha + \phi_\beta - 2\Psi_2^{\text{TPC}}) \rangle$$

$$\Delta\gamma = \gamma_{112}(\text{OS}) - \gamma_{112}(\text{SS})$$

$$\delta \equiv \langle \cos(\phi_\alpha - \phi_\beta) \rangle$$

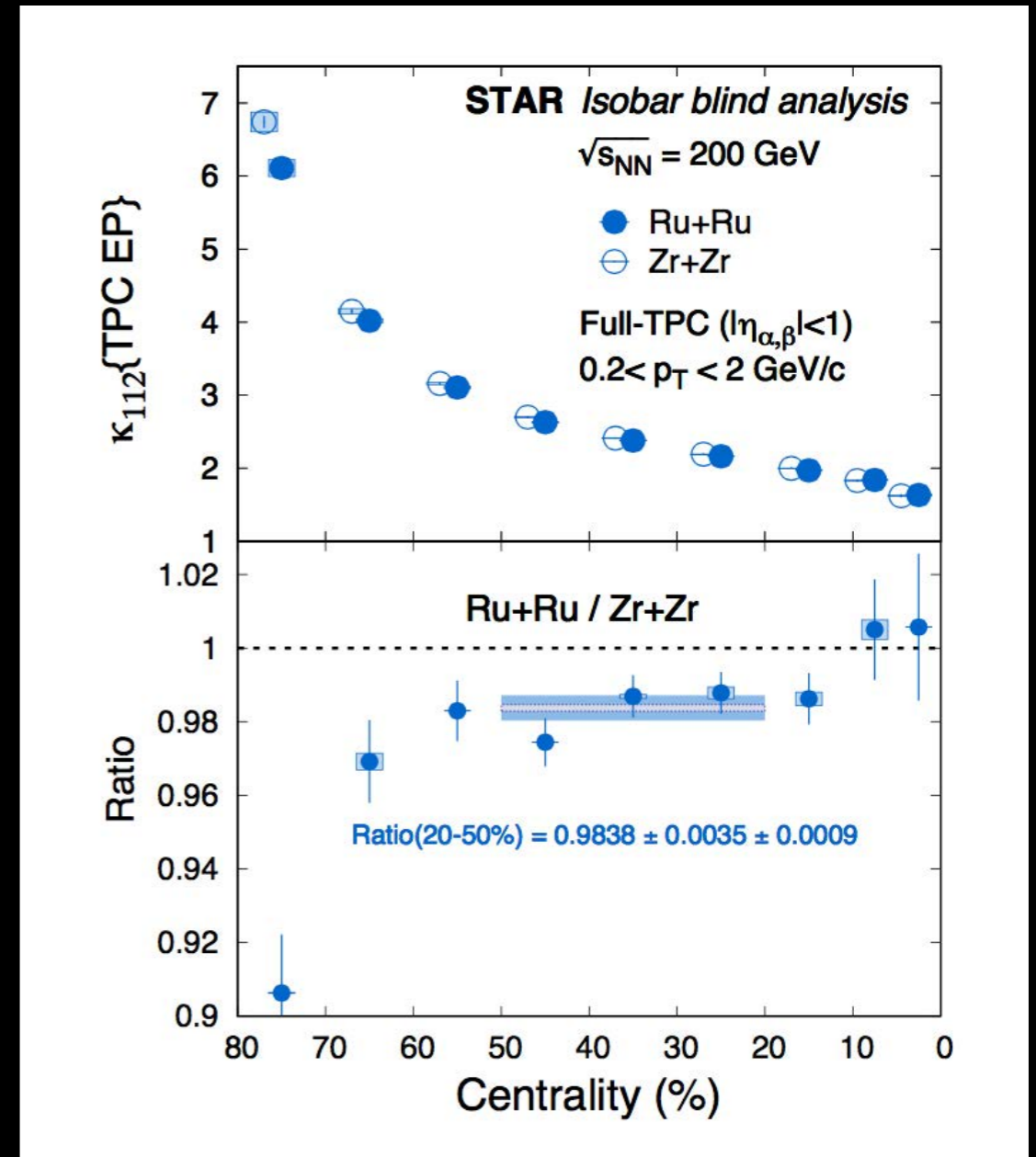
$$\Delta\delta = \delta(\text{OS}) - \delta(\text{SS})$$

Factorization breaking:

$$\kappa_{112} \equiv \frac{\Delta\gamma_{112}}{v_2 \cdot \Delta\delta}$$

Pre-defined CME criteria:

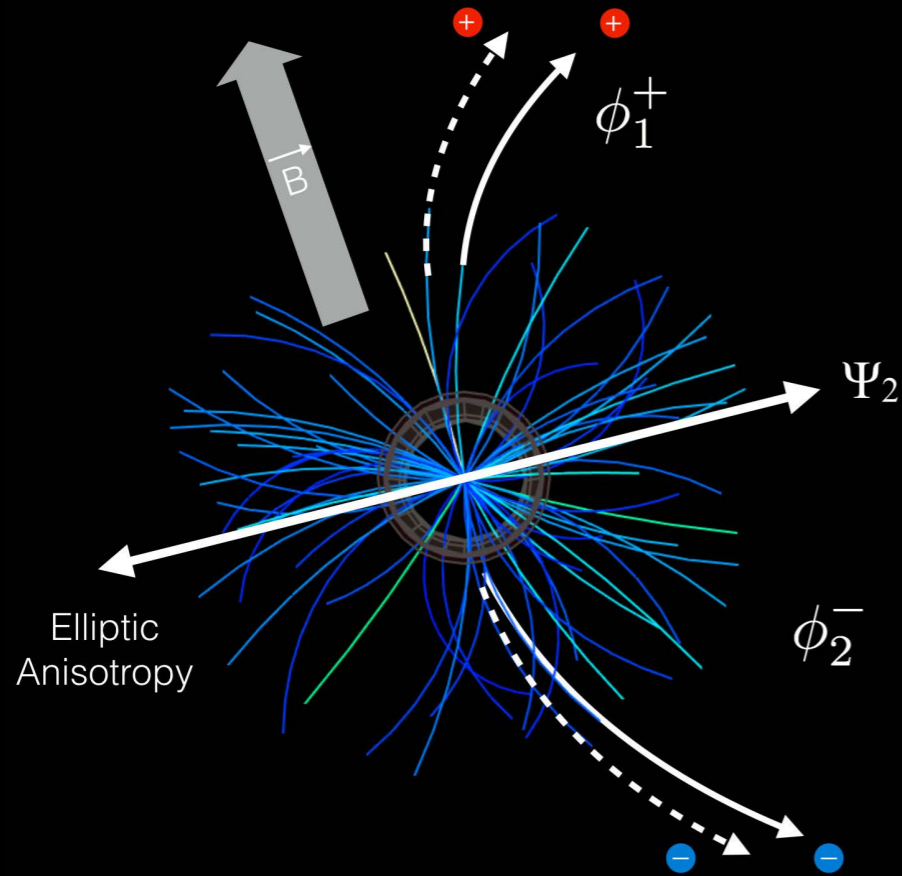
$$\frac{\kappa_{112}^{\text{Ru+Ru}}}{\kappa_{112}^{\text{Zr+Zr}}} > 1$$



This pre-defined CME signature is NOT seen

# Charge separation across triangular flow plane

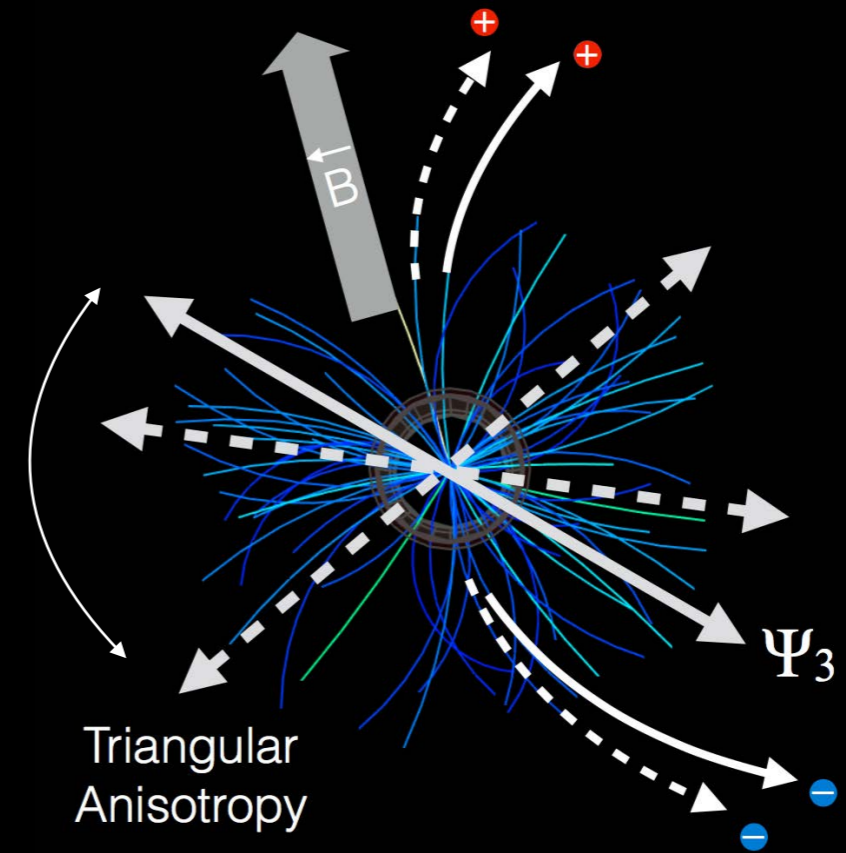
B-field is corrected to  $\Psi_2$  plane



$$\gamma_{112} = \langle \cos(\phi_\alpha + \phi_\beta - 2\Psi_2) \rangle$$

Signal (B-field) + Background ( $\propto v_2$ )

B-field is not-corrected to  $\Psi_3$  plane

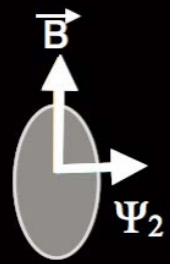


$$\gamma_{123} = \langle \cos(\phi_\alpha + 2\phi_\beta - 3\Psi_2) \rangle$$

Background only ( $\propto v_3$ )

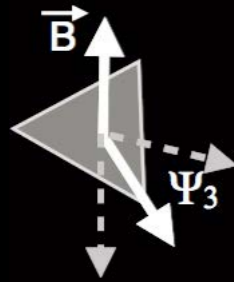
Charge separation across third harmonic plane can serve as data-driven baseline

# Charge separation across $\Psi_2$ and $\Psi_3$ planes



$$\gamma_{112} = \langle \cos(\phi_1^\alpha + \phi_2^\beta + 2\Psi_2) \rangle$$

signal + background

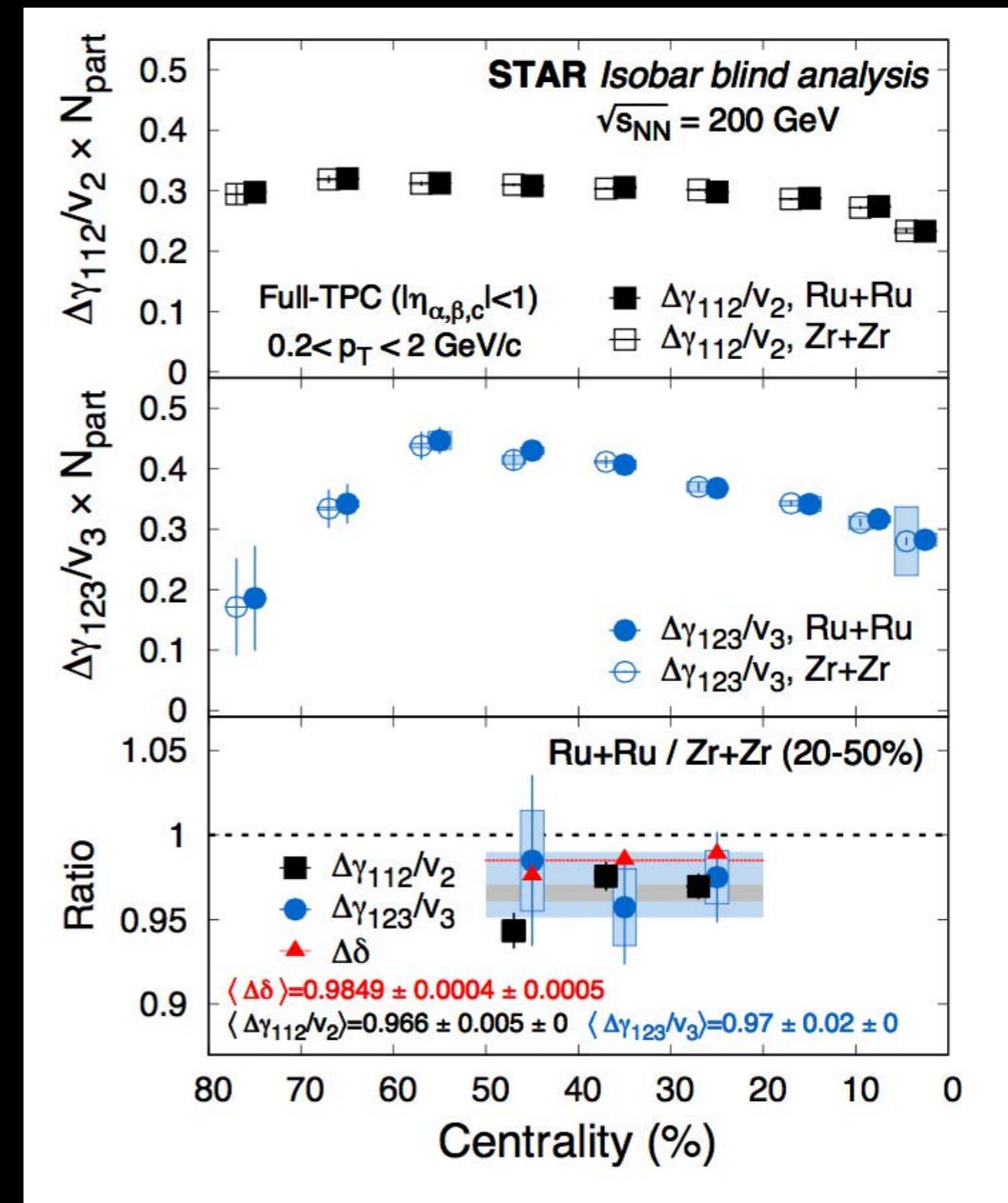


$$\gamma_{123} = \langle \cos(\phi_1^\alpha + 2\phi_2^\beta - 3\Psi_3) \rangle$$

100% background

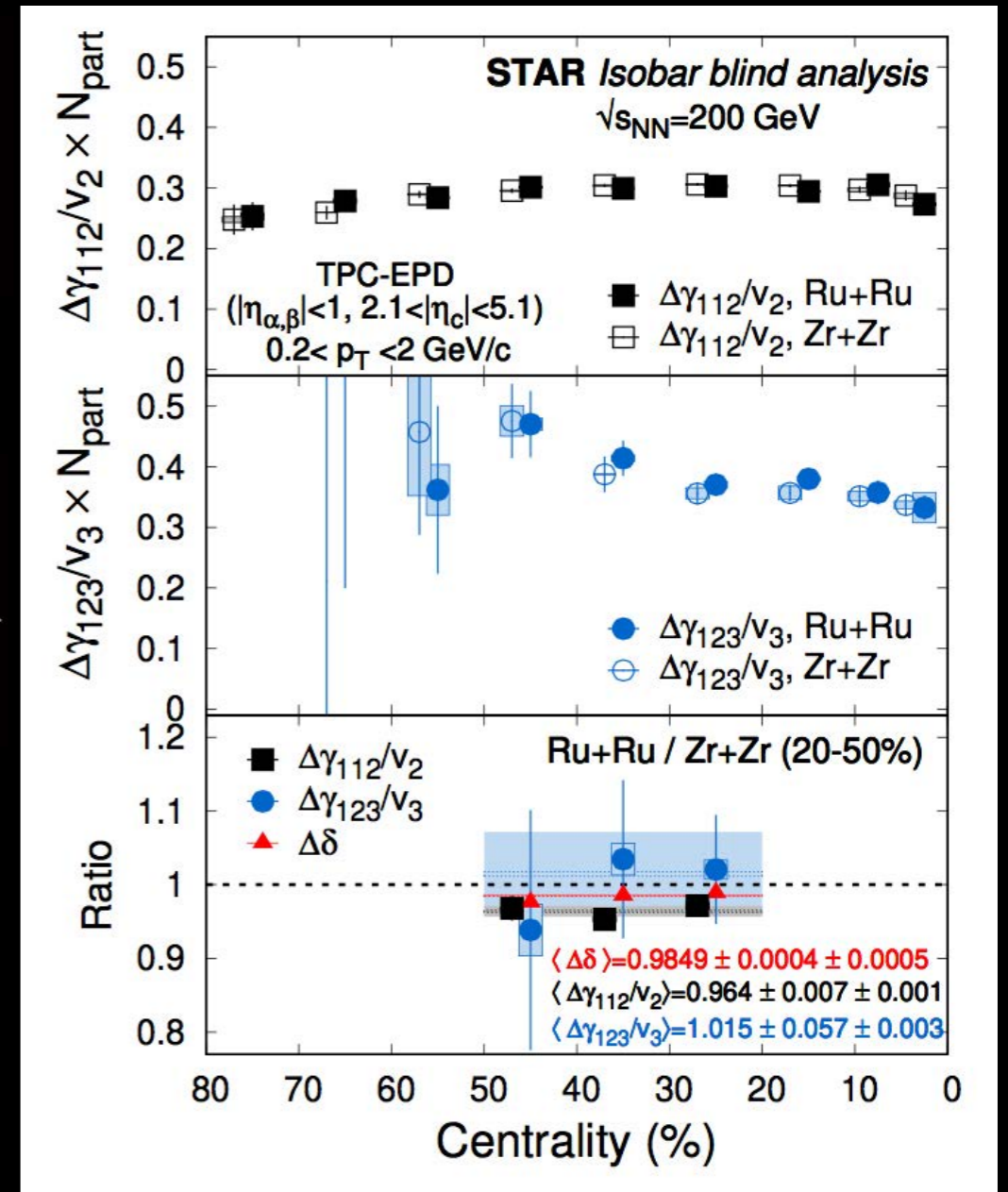
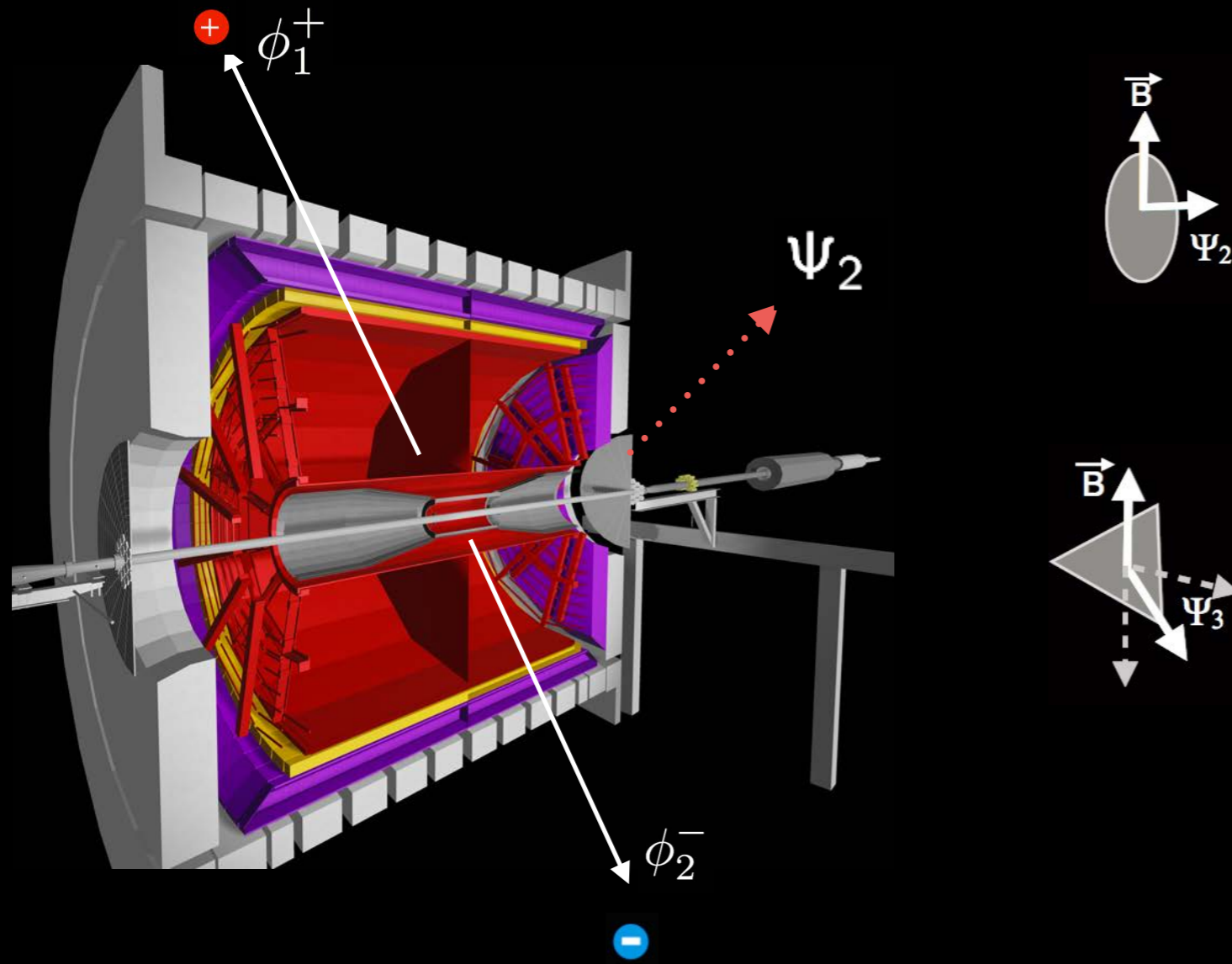
Pre-defined CME criteria:

$$\frac{(\Delta\gamma_{112}/v_2)^{RuRu}}{(\Delta\gamma_{112}/v_2)^{ZrZr}} > \frac{(\Delta\gamma_{123}/v_3)^{RuRu}}{(\Delta\gamma_{123}/v_3)^{ZrZr}}$$



This pre-defined CME signature is NOT seen

# Measurement using STAR EPD (for the first time)



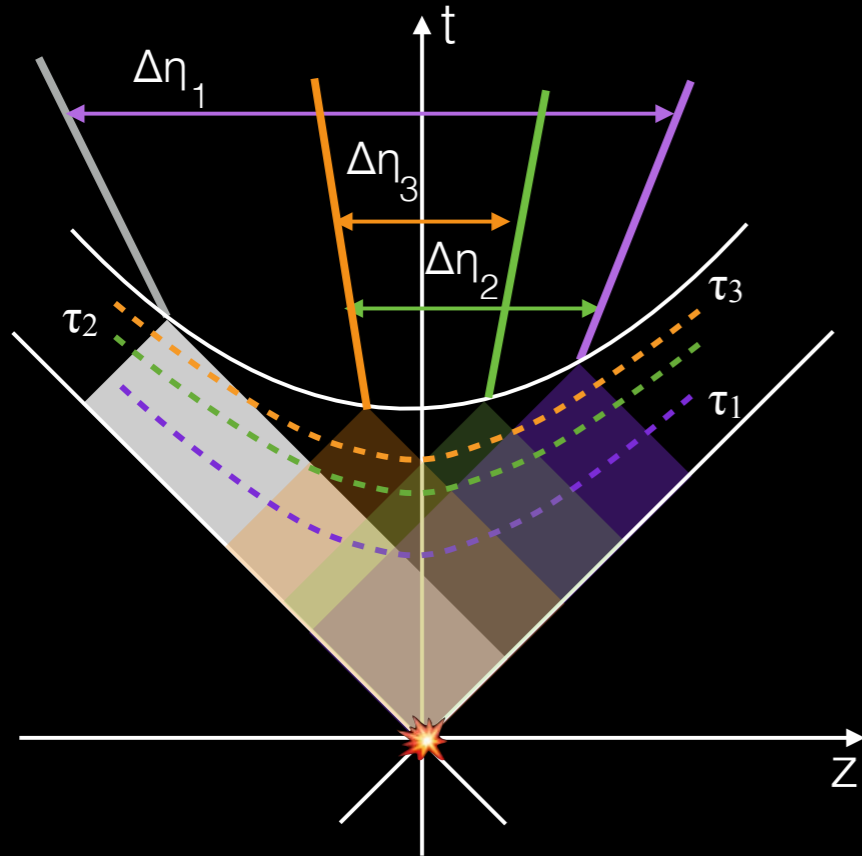
Pre-defined CME criteria:

$$\frac{(\Delta\gamma_{112}/v_2)^{RuRu}}{(\Delta\gamma_{112}/v_2)^{ZrZr}} > \frac{(\Delta\gamma_{123}/v_3)^{RuRu}}{(\Delta\gamma_{123}/v_3)^{ZrZr}}$$

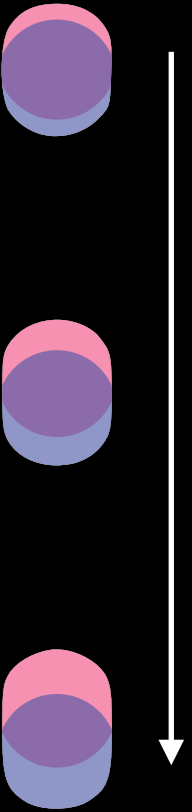
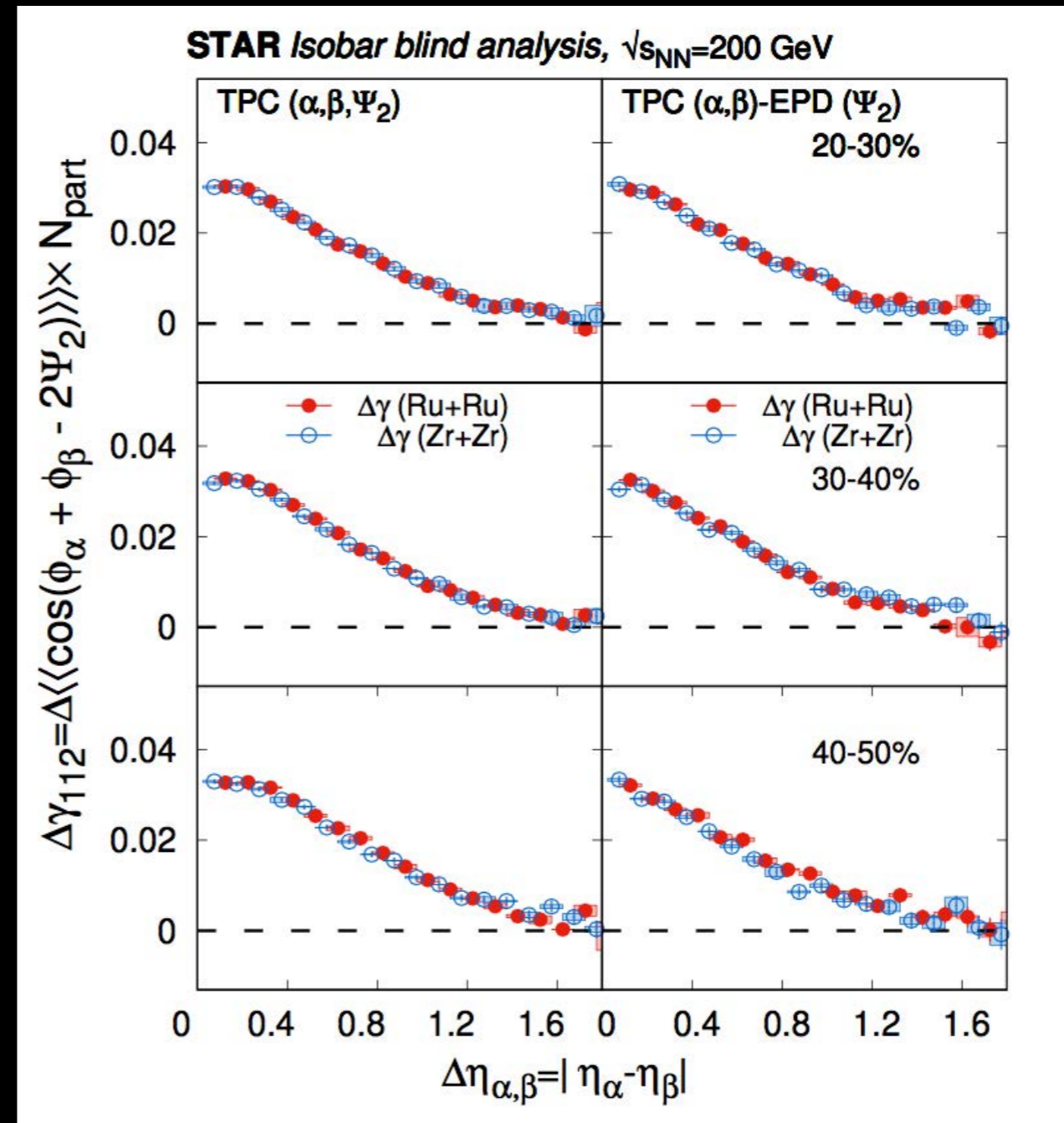
This pre-defined CME signature is NOT seen

# Relative pseudorapidity dependence of $\gamma_{112}$

Causality precludes late-time correlations to spread over large  $\eta$  (wide acceptance  $\rightarrow$  strength)

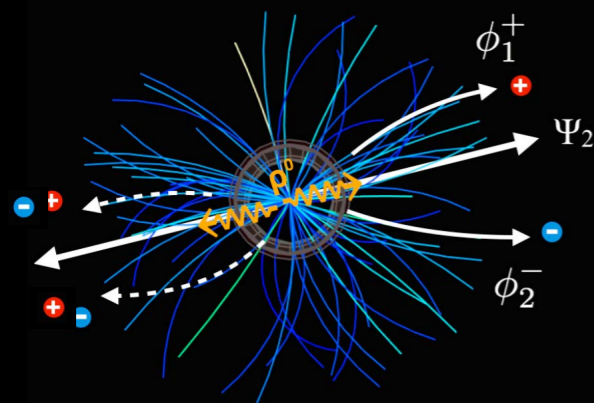
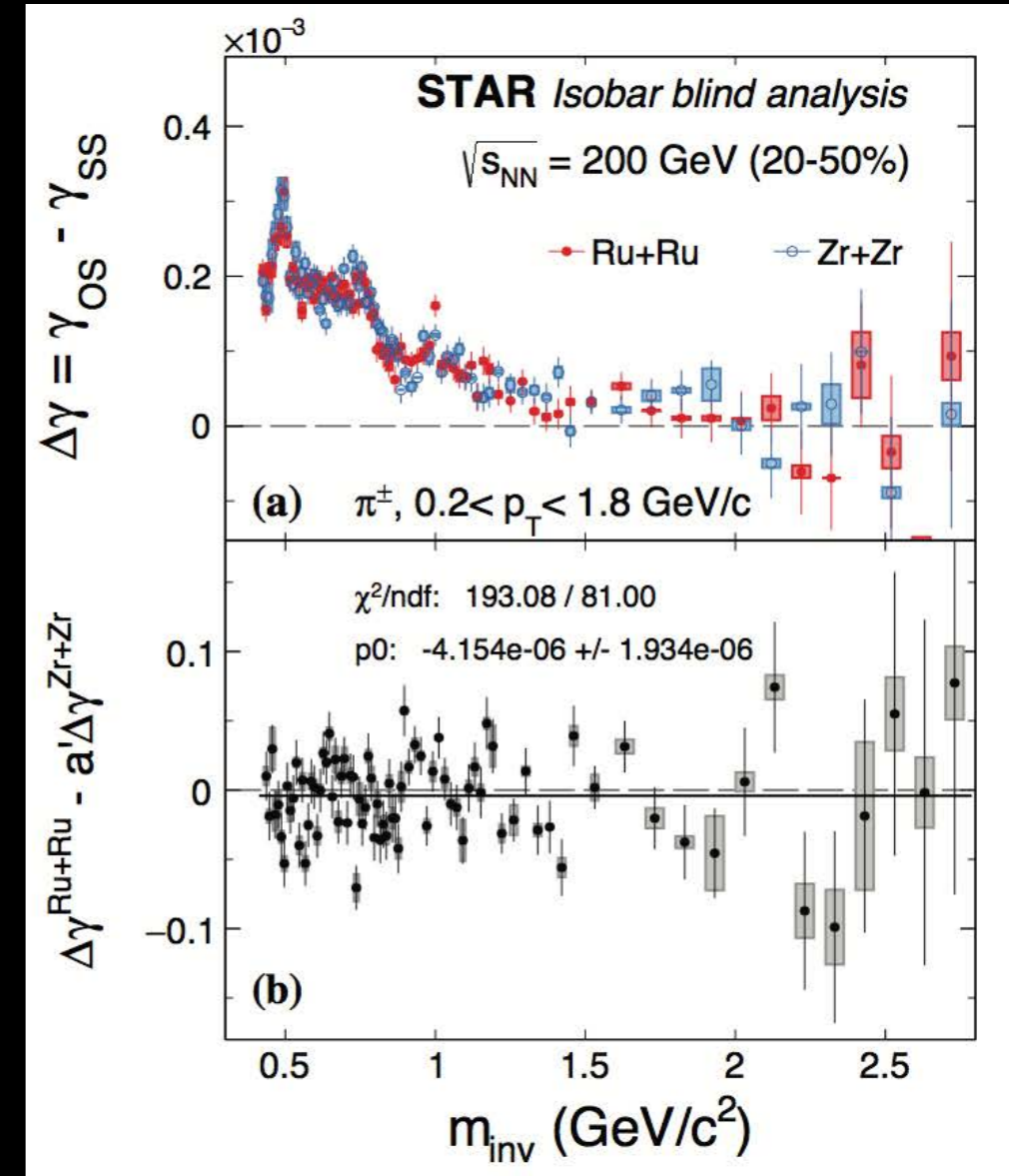
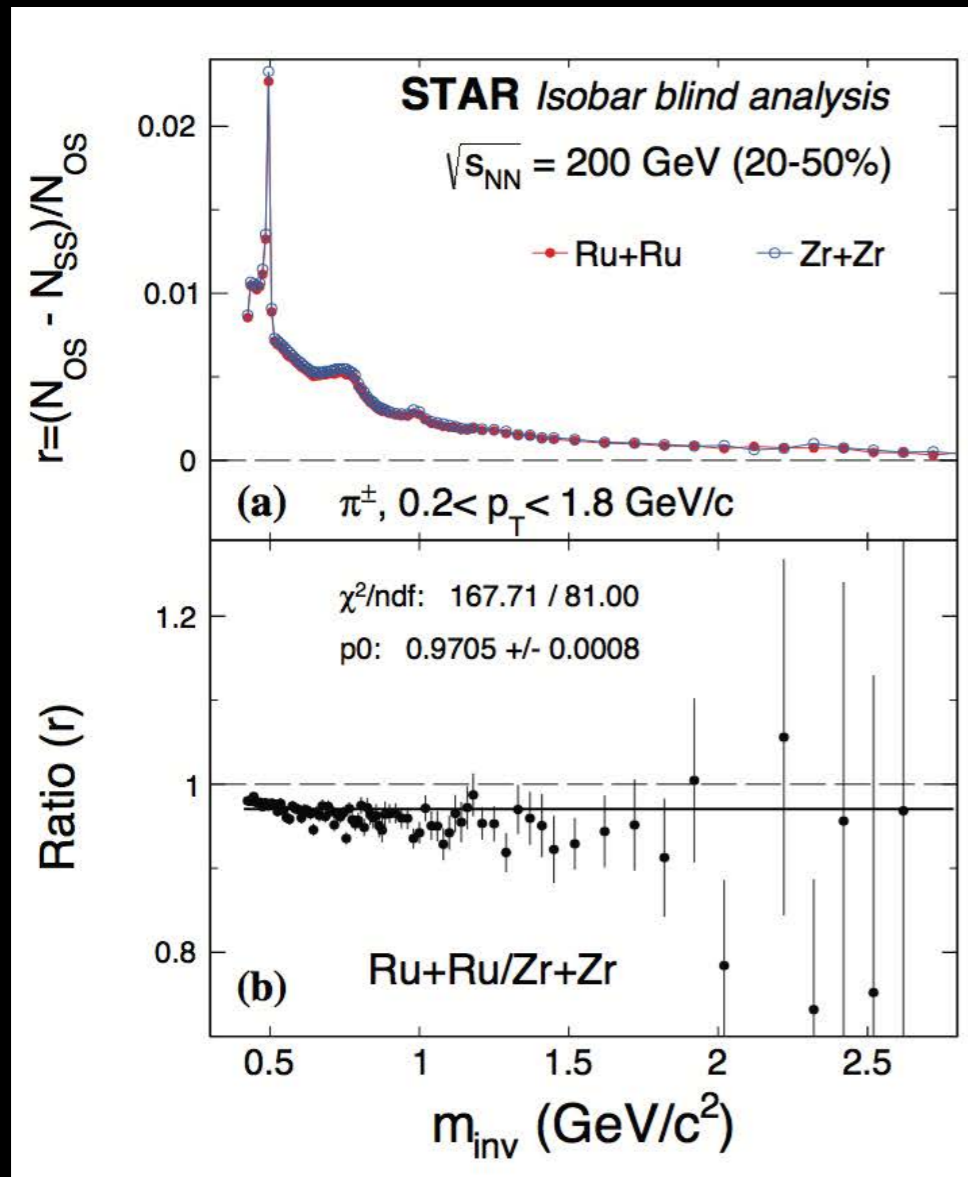


B-field driven charge separation:  
large  $\Delta\eta > 1$   
Resonance decay: smaller  $\Delta\eta < 1$



The relative pseudorapidity dependence is similar between the two species

# Invariant mass dependence of $\gamma_{112}$



Resonances are identifiable as peaks in invariant mass distribution

Pre-defined CME criteria:

$$\Delta\gamma^{\text{Ru+Ru}} - a' \Delta\gamma^{\text{Zr+Zr}} > 0$$

$$a' = v_2^{\text{Ru+Ru}} / v_2^{\text{Zr+Zr}}$$

This pre-defined signature is NOT seen

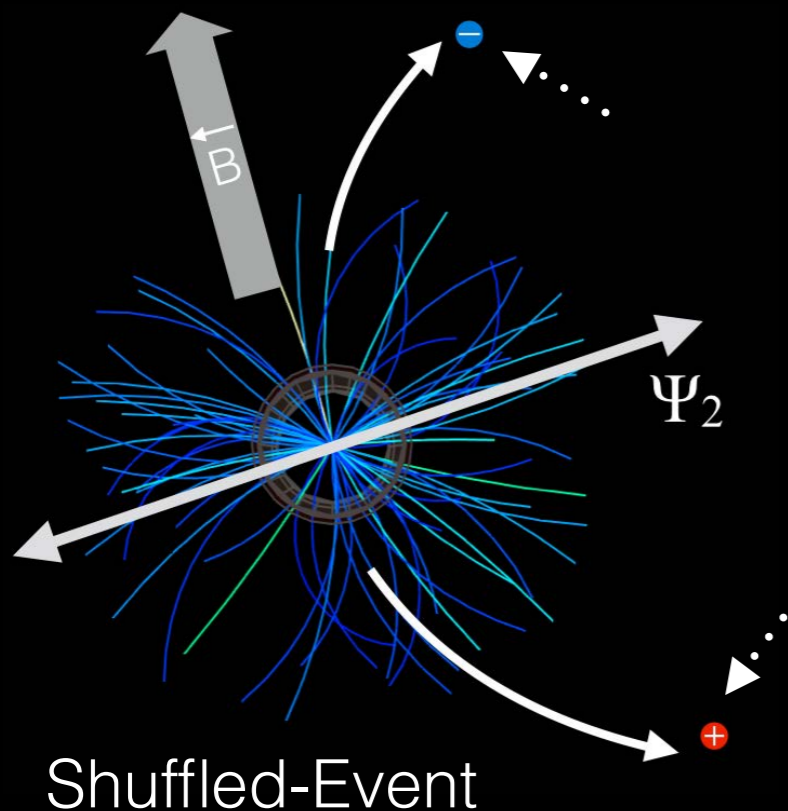
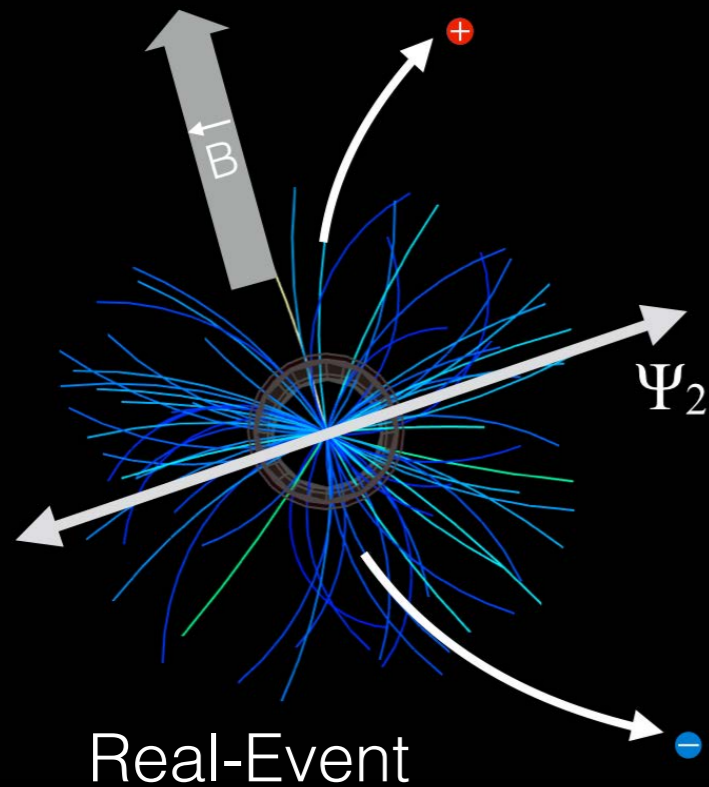
# Alternate charge separation measure: R-variable

R-variable is a ratio of distribution  
(of event-by-event charged-dependent dipole anisotropy)

$$R_{\Psi_2}(\Delta S) = C_{\Psi_2}(\Delta S) / C_{\Psi_2}^{\perp}(\Delta S),$$

$$C_{\Psi_2}(\Delta S) = \frac{N_{\text{real}}(\Delta S)}{N_{\text{shuffled}}(\Delta S)},$$

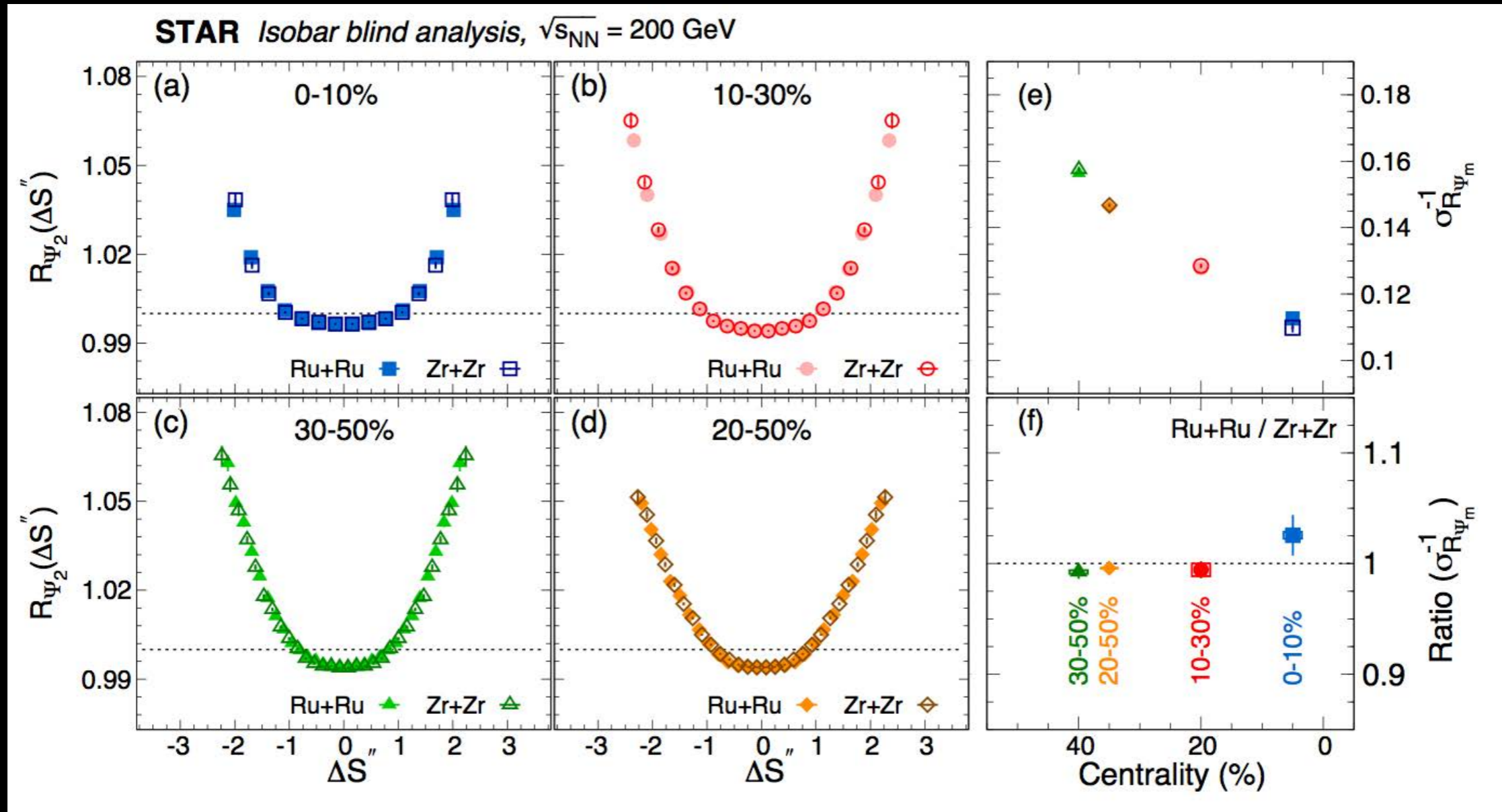
$$\Delta S = \frac{\sum_1^{n^+} w_i^+ \sin(\Delta\varphi_2)}{\sum_1^{n^+} w_i^+} - \frac{\sum_1^{n^-} w_i^- \sin(\Delta\varphi_2)}{\sum_1^{n^-} w_i^-},$$



The width of R-variable is sensitive to signal + Background

The case for CME is:  $1/\sigma_{R_{\Psi_2}}(Ru + Ru) > 1/\sigma_{R_{\Psi_2}}(Zr + Zr)$

# Alternate charge separation measure: R-variable

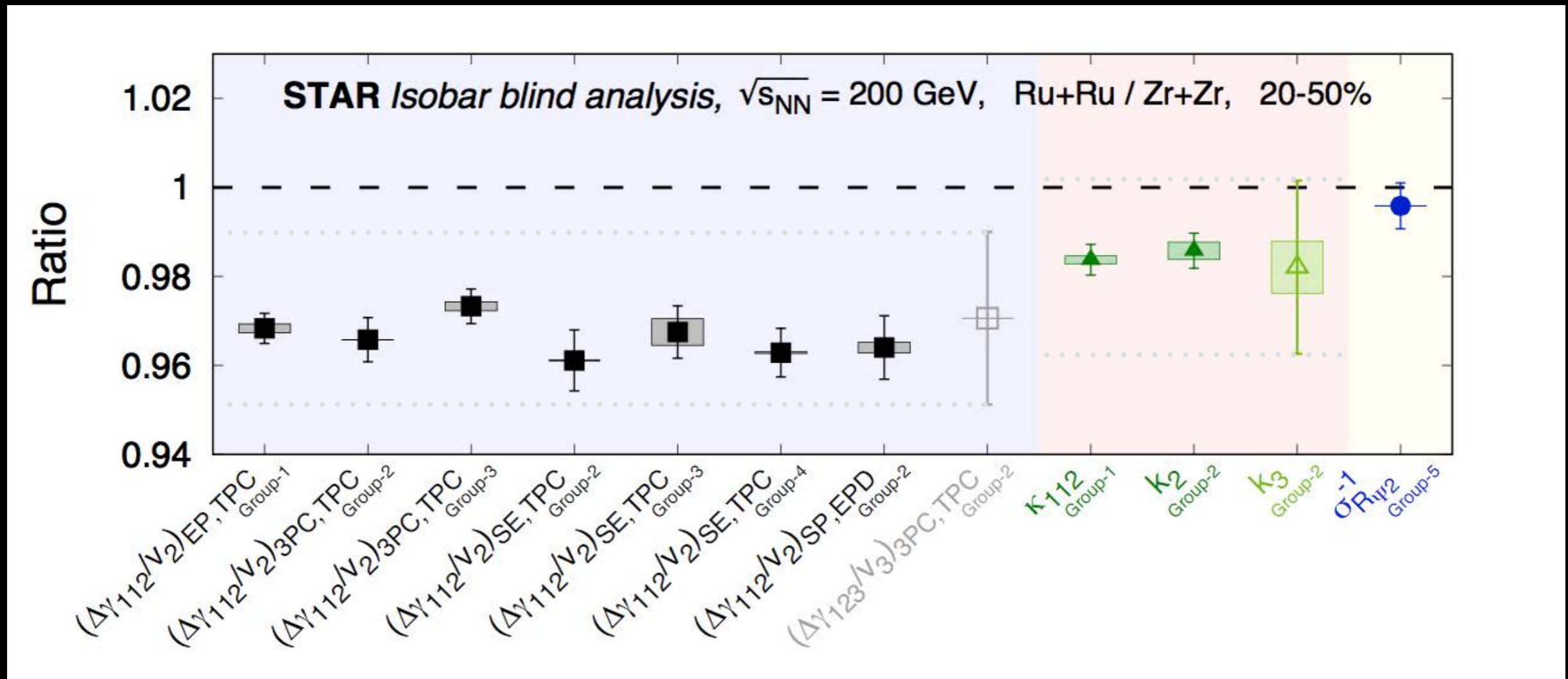


Pre-defined CME criteria:  $1/\sigma_{R_{\Psi_2}}(\text{Ru} + \text{Ru}) > 1/\sigma_{R_{\Psi_2}}(\text{Zr} + \text{Zr})$

This pre-defined signature is NOT seen



# Compilation of all the results

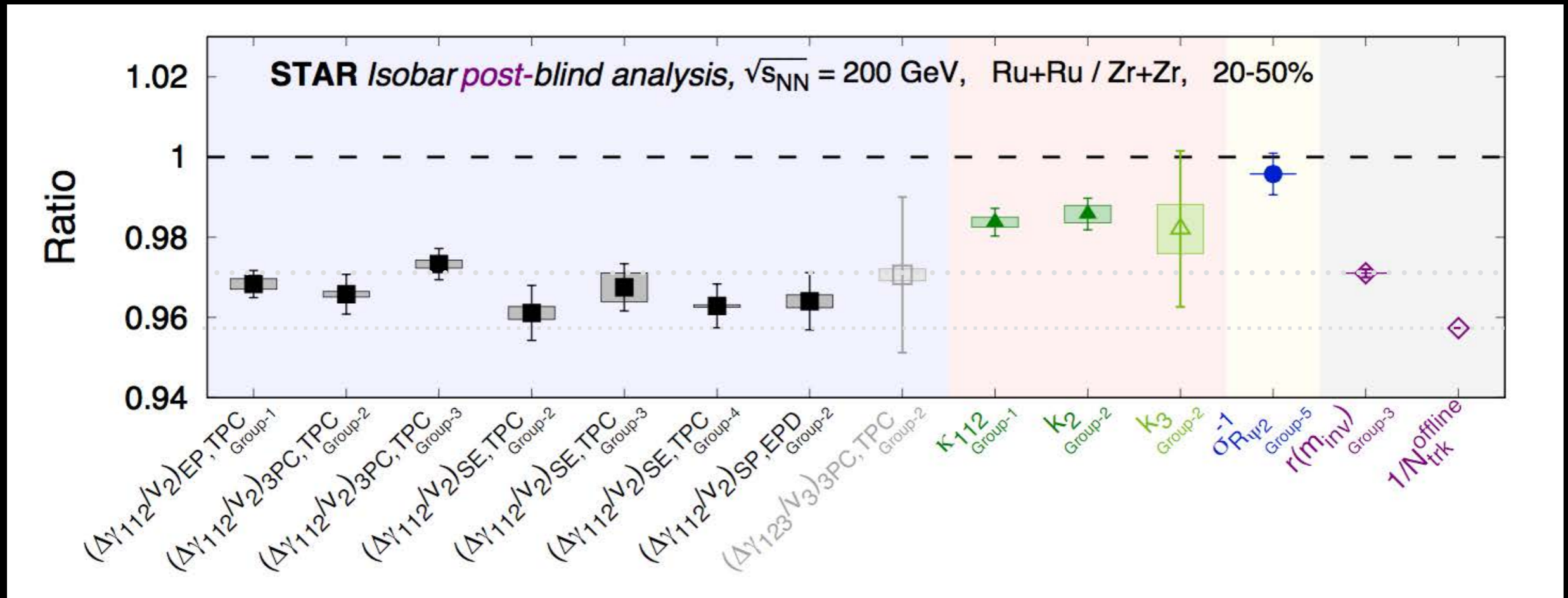


Good consistency between results from different groups.

Predefined CME signatures: Ratios involving  $\Psi_2 >$  those involving  $\Psi_3$ , and  $> 1$

None of the predefined signatures have been observed in the blind analysis

# Postblinding



Why ratios of  $\Delta\gamma/v_2$  are below unity?

Inverse of multiplicities, or as an alternative  $r$  maybe better baselines compared to unity used in the pre-defined blind analysis documentation

Alternate baselines also do not present a clear case for CME

# Conclusion

Experimental test of CME in isobar collisions performed using a blind analysis

Multiplicity distributions and mean multiplicity are different between isobars

$v_2$  (2.5%) &  $v_3$  (7%) difference between the isobars seen in central events

A precision down to 0.4% achieved in the primary CME variable

All criteria to observe CME were pre-defined and none observed

CME observables  $\Delta\gamma/v_2$  baseline are affected by the multiplicity difference (4% in 20-50%), post-blind analysis compared two possibilities, no clear case for CME

The observed multiplicity difference between the isobars requires future CME analyses to better understand the baselines in order to best utilize the precision demonstrated in this analysis. Better understanding of the non-flow may be another goal.